4

Oscillatory Phenomena as a Probe to Study Pitting Corrosion of Iron in Halide-Containing Sulfuric Acid Solutions

Dimitra Sazou*, Maria Pavlidou,
Aggeliki Diamantopoulou and Michael Pagitsas**
Department of Chemistry, Aristotle University of Thessaloniki, Thessaloniki Greece

1. Introduction

Oscillatory phenomena and other nonlinear phenomena such as bistability and spatiotemporal patterns are frequently observed in metal and alloy electrodissolution-passivation processes (Hudson & Tsotsis, 1994; Koper, 1996a; Krischer, 1999; Krischer, 2003b). Current oscillations during the Fe electrodissolution-passivation in acid solutions were reported as early as 1828 (Fechner, 1828). Since then, metal|electrolyte interfacial systems have received considerable interest over the past three decades for many reasons. Among them, is that progress in the theory of nonlinear dynamical systems, achieved in parallel over last decades, has led to the formulation of new theoretical concepts and tools that could apply to electrochemical oscillators. Therefore, an understanding of the fundamental principles underlying the nonlinear phenomena observed in electrochemical processes has been considerably improved (Berthier et al., 2004; Eiswirth et al., 1992; Karantonis & Pagitsas, 1997; Karantonis et al., 2005; Karantonis et al., 2000; Kiss & Hudson, 2003; Kiss et al., 2003; Kiss et al., 2006; Krischer, 2003b; Parmananda et al., 1999; Parmananda et al., 2000; Sazou et al., 1993a). On the other hand, electrochemical systems can be readily controlled through the variation of the potential (under current-controlled conditions) or the current (under potential-controlled conditions) and have served as experimental model systems to implement and test new theoretical concepts.

Technological applications of nonlinear electrochemical phenomena in materials science are exemplified by their impact on electrodissolution, electrodeposition and electrocatalytic reactions (Ertl, 1998; Ertl, 2008; Nakanishi et al., 2005; Orlik, 2009; Saitou & Fukuoka, 2004). Another promising application might be the preparation of self-organized nanostructures such as TIO_2 nanotubes (Taveira et al., 2006). Regarding electrodissolution processes, the progress in defining the conditions for metal stability and dynamical transitions in metal|electrolyte systems is of fundament importance for metal performance and safety in natural environments (Hudson & Basset, 1991; Lev et al., 1988; Sazou et al., 2000b; Sazou et

* Corresponding author
** Deceased 26 April 2009.

al., 1993a; Sazou & Pagitsas, 2003b). The existence of passivity on metals is well recognized as the most important factor for the metal safe use in our metal-based civilization (Sato, 1990; Schmuki, 2002; Schultze & Lohrenger, 2000). It has been shown that depassivating factors, resulting either in uniform dissolution of passive films (general corrosion) or localized breakdown of an otherwise stable passivity on metals (pitting corrosion) give rise to temporal as well as spatiotemporal instabilities (Green & Hudson, 2001; Otterstedt et al., 1996; Sazou & Pagitsas, 2003b; Sazou et al., 2009; Wang et al., 2004). For Fe, these instabilities are more pronounced in pitting corrosion occurring in different corrosive media, but mostly, in those containing halides such as chlorides, bromides and iodides. This will be the main theme of this brief review.

In practice, chlorides are of a major concern due to their abundance in environments encountered in industry and in domestic, commercial and marine industry. Extensive studies have been carried out over the last century and continue aiming to estimate the conditions leading to local breakdown, gain a deeper understanding of mechanisms and processes underlying pitting and develop effective strategies of metal protection (Bohni, 1987; Frankel, 1998; Kaesche, 1986; Macdonald, 1992; Sato, 1982; Sato, 1989; Sato, 1990; Strehblow, 1995). Exploring the nonlinear dynamical phenomena associated with pitting corrosion of Fe and other metals might provide a new approach in investigating passivity breakdown from both mechanistic and kinetic points of view. Especially, electrochemical measurements and nonlinear dynamics in conjunction with new surface analytical techniques constitute a promising way towards studying pitting corrosion (Maurice & Marcus, 2006; Wang et al., 2004).

The onset of current and potential oscillations is the most common nonlinear behavior of the Fe|electrolyte system in acidic solutions containing halides, X^- ($X^- \equiv Cl^-$, Br^-, I^-) (Georgolios & Sazou, 1998; Koutsaftis et al., 2007; Li et al., 2005; Ma et al., 2003; Pagitsas & Sazou, 1999; Sazou et al., 2000a; Sazou et al., 2000b; Sazou et al., 1993b; Sazou et al., 1992). In particular, it was shown that adding small amounts of X^- in the Fe|*n* M H_2SO_4 system induces complex periodic and aperiodic current oscillations under potential-controlled conditions (Georgolios & Sazou, 1998; Koutsaftis et al., 2007; Li et al., 2005; Pagitsas & Sazou, 1999; Sazou et al., 2000a; Sazou et al., 2000b). These oscillations are of large amplitude and represent passive-active events emerged out of an extensive potential region. A gradual increase of halide concentration results in the establishment of a limiting current region out of the Fe passive state. This new state of Fe is accompanied by complex aperiodic current oscillations of small amplitude. The latter oscillations occur under mass-transport controlled conditions, which are established inside pits due to the formation of ferrous salt layers (Sazou & Pagitsas, 2003a; Sazou & Pagitsas, 2006a). Moreover, as was mentioned above, halides induce also potential oscillations under current-controlled conditions, associated with either early (Postlethwaite & Kell, 1972; Rius & Lizarbe, 1962; Sazou et al., 2009) or late stages (Li & Nobe, 1993; Li et al., 1993; Li et al., 1990; Strehblow & Wenners, 1977) of pitting corrosion.

Unambiguously, both current and potential oscillations include valuable information related to the kinetics of the oxide growth and its breakdown (Pagitsas et al., 2001; Pagitsas et al., 2002; Sazou & Pagitsas, 2003a; Sazou & Pagitsas, 2006a). Though, several investigations aiming to reveal and use profitably this information have been brought about some progress in understanding underlying processes, many aspects remain to be revealed and exploited.

In this article only few of these aspects will be touched upon. Emphasis is placed on displaying certain features of the oscillatory response of the halide-containing Fe|*n* M H_2SO_4 system that might be employed in establishing new tools, useful in detecting and characterizing the extent of pitting corrosion on passive Fe surfaces.

The chapter starts with a short section (section 2) in which basic information about measurements used in all sections is provided.

In section 3, the basics regarding the origin of oscillations in metal|electrolyte systems under corrosion conditions are discussed briefly to show that the halide-free Fe|*n* M H_2SO_4 system, being an N-NDR oscillator, is unlikely to display either current oscillations within the stable passive state, extended beyond the Flade potential, or potential oscillations under galvanostatic conditions. Thus oscillatory phenomena discussed in this chapter are the result of the interplay between pitting corrosion and basic dynamics of an N-NDR system that is transformed rather to an HN-NDR oscillator.

Section 4, displays briefly the characteristic current-potential, $I = f(E)$ or potential-current, $E = f(I)$ polarization curves of the halide-free Fe|0.75 M H_2SO_4 system traced under potentiodynamic and galvanodynamic conditions, respectively. This section aims in demonstrating that in the absence of aggressive ions only single periodic oscillations occur. The fundamental physico-electrochemical processes underlying the mechanism of single periodic oscillations are briefly summarized.

Section 5, focuses on the nonlinear dynamics of the halide-perturbed Fe|0.75 M H_2SO_4 system at relatively low halide concentrations. Halide-induced changes in $I = f(E)$ and $E = f(I)$ polarization curves are pointed out. By choosing appropriate potential and current values from $I = f(E)$ and $E = f(I)$ curves, current and potential time-series are traced under potentiostatic and galvanostatic conditions, respectively. Experimental results are analyzed in order to establish appropriate kinetic quantities as a function of either the potential or current and the halide concentration. Emphasis is placed here on how these quantities can be used in studying initiation of pitting at early stages.

Section 6, provides selected experimental examples displaying the nonlinear response of the halide-containing Fe|0.75 M H_2SO_4 system at relatively high halide concentrations. It is thus concerned with late stages of pitting corrosion, which are exemplified by a different type of oscillations.

Section 7, includes an overview of conditions under which the nonlinear response of the halide-containing Fe|0.75 M H_2SO_4 system appears and a summary of proposed diagnostic criteria, appropriate for characterization of pit initiation and its growth.

In section 8, conclusions are presented, while section 9 contains references.

2. Experimental

Electrochemical measurements were carried out using a VoltaLab 40 electrochemical system and the VoltaMaster 4 software from Radiometer Analytical. Additionally, a Wenking POS 73 potentioscan from Bank Elektronik was employed. It was interfaced with a computer, which was equipped with an analog-to-digital, and vice versa, converter PCL-812PG enhanced multi-Lab. Card (Advantech Co. Ltd). The maximum sampling rate of the PCL-

812PG card was equal to 30 kHz. The working electrode (WE) was the cross section of an iron wire with a diameter equal to 3 mm from Johnson Matthey Chemicals (99.9%) embedded in a 1 cm diameter PTFE cylinder (surface area=0.0709 cm^2). A volume of 150 ml was maintained in a three-electrode electrochemical cell. A Pt sheet (2.5 cm^2) and a saturated calomel electrode (SCE) were used as the counter (CE) and reference electrodes (RE), respectively. The Fe-disc surface was polished by wet sand papers of different grit size (100, 180, 320, 500, 800, 1000, 1200 and superfine) and cleaned with twice-distilled water in an ultrasonic bath. Solutions were prepared with H_2SO_4 (Merck, pro-analysis 96% w/w) and NaF or NaCl or NaBr or NaI, all from Fluka (puriss p.a.), using twice-distilled water. Measurements were carried out at 298 K, while N_2 was passed above the solution during the course of the experiment. A scanning electron microscope (SEM) JEOL JSM-840A was used for the Fe surface observation. Further experimental details can be found in previous studies (Pagitsas et al., 2003; Sazou & Pagitsas, 2003b; Sazou et al., 2009).

3. Origin of oscillations in corroding metal|electrolyte interfacial systems

Spontaneous oscillatory phenomena observed in metal electrodissolution-passivation reactions are often associated with multisteady-state current-potential (*I-E*) curves due to the occurrence of a region with negative differential resistance (NDR). NDR appears either in N-type (the electrode potential acts as activator, positive feedback variable) (Fig. 1) or S-type (the electrode potential acts as inhibitor, negative feedback variable) *I-E* curves (Fig. 2).

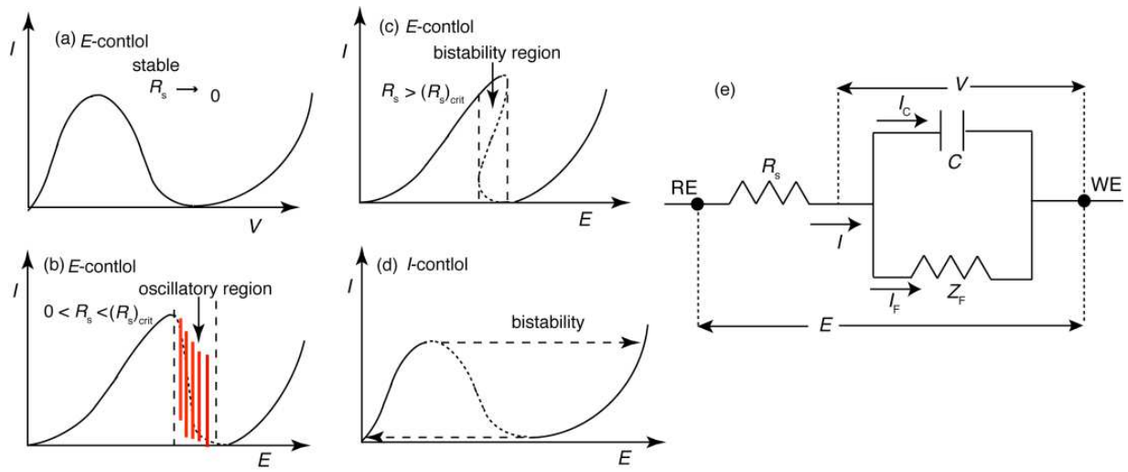

Fig. 1. Multisteady-state current-potential curves of N-type under potential controlled conditions with (a) a stable NDR-region at vanishing R_s, (b) current oscillations around NDR for intermediate values of R_s, (c) bistability without oscillations. (d) N-type curve under current-controlled conditions with bistability but without potential oscillations. (e) A general equivalent circuit of an electrochemical cell where E is the applied potential and V is the electrode potential.

Three basic categories are suggested to classify homogeneous (the spatial coupling is neglected) electrochemical oscillators. (Koper, 1996b; Krischer, 2003a):

1. N-NDR, characterized by an N-type current-potential curve for a vanishing ohmic resistance, $R_s \rightarrow 0$ (Fig. 1a). Potentiostatic current oscillations occur for intermediate

values of R_s (Fig. 1b) whereas bistability without oscillations exists for $R_s > (R_s)_{crit}$ (Fig. 1c). Galvanostatic potential oscillations do not occur (Fig. 1d). The majority of corroding metal|electrolyte systems that exhibit current oscillations across the active-to-passive transition are related to N-NDR systems. Among them the Fe|H_2SO_4, Fe|H_3PO_4 Co|H_3PO_4 and Zn|NaOH systems being few of them (Hudson & Tsotsis, 1994).

2. HN-NDR, characterized by a regime of a hidden negative differential resistance in the *I-E* polarization curve. Potentiostatic current oscillations around a regime of a positive slope occur when $R_s>(R_s)_{crit}$ whereas galvanostatic potential oscillations occur as well. Example of this category is the transpassive electrodissolution of Ni in H_2SO_4 (Lev et al., 1988).
3. S-NDR, characterized by an S-type polarization curve (Fig. 2). S-NDR systems oscillate under galvanostatic conditions at applied current values located within the NDR regime of the polarization curve. Example of this category may include the complicated dynamics of the electrodissolution of Fe in concentrated nitric acid (Gabrielli et al., 1976).

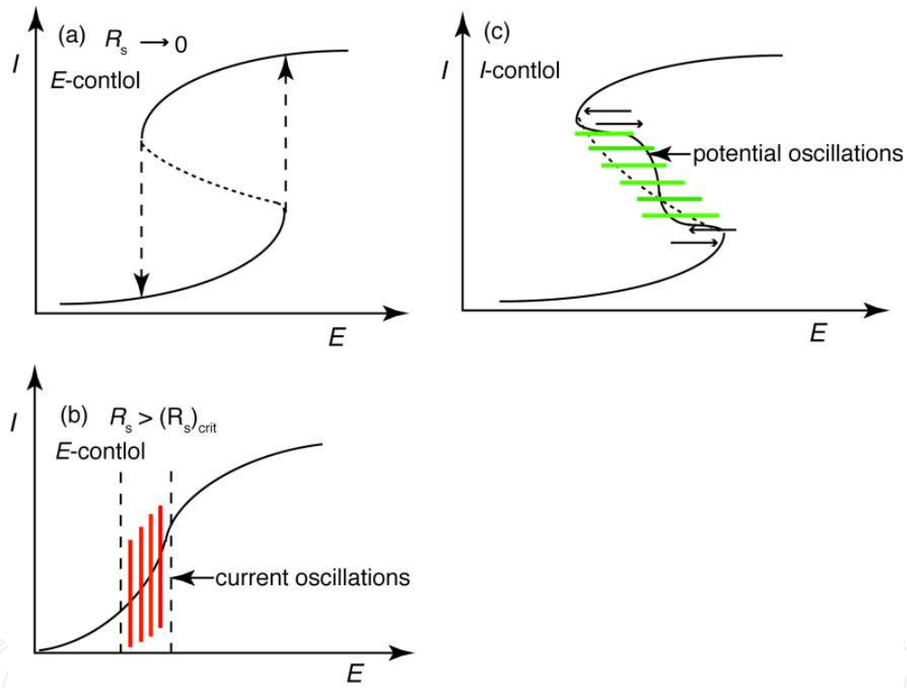

Fig. 2. Multisteady-state current-potential curves of S-type under potential-controlled conditions with (a) a vanishing R_s, (b) current oscillations for $R_s>(R_s)_{crit}$. (c) Potential oscillations under current-controlled conditions within the NDR regime, which in practice becomes not accessible and the *I-E* curve exhibits bistability.

As was shown in Fig. 1, the NDR in N-type current-potential curves is destabilized by increasing the ohmic resistance, R_s. Considering the general equivalent circuit (EC) of an electrochemical cell (Fig. 1e), the R_s represents the ohmic resistance, which includes un uncompensated cell resistance and a resistor connected in series between the working electrode, WE and ground. The total current I through the electrolyte interface consists of the faradaic current, I_F through the faradaic impedance, Z_F, and the current, I_C through the capacitor, C of the double layer. Under potential-controlled conditions, the potential, E

between the WE and reference electrode (RE) should be constant and equal to $E=V + IR_s$. Destabilization of the N-type curves might be caused through the variation of the electrode potential, V. It introduces a positive feedback loop (activator) in the system by increasing R_s, which is used as a bifurcation parameter. Bifurcation parameter is a system parameter, which induces changes in the dynamic behavior of the system at a critical value. Dynamical changes occur through bifurcations (Koper, 1996b; Koper & Sluyters, 1993b).

Elucidation of the origin of oscillations includes the effect of the ohmic potential drop, IR_s and the discontinuous variation of the surface coverage ratio with the electrode potential due to the formation-dissolution of anodic surface films or the presence of autocatalytic chemical reactions concurrently occurring with electron transfer reactions. Mechanistically, the faradaic impedance, Z_F, depicted in the EC of an electrochemical cell (Fig. 1e), is related to the electrochemical processes at the metal (WE)|interface. Z_F should be derived from a reaction scheme. The basic equations are the mass balance for the reaction intermediates and charge balance equations derived from the general EC shown in Fig. 1e.

$$\frac{\mathrm{d}c_i}{\mathrm{d}t} = f_i(c_i, V) \tag{1}$$

$$\frac{\mathrm{d}V}{\mathrm{d}t} = \frac{I - I_F(V)}{CA} \tag{2}$$

where c_i is the surface concentration of reaction intermediates and A is the surface area. At least one intermediate species, which introduces a negative feedback loop (inhibitor), is required for an N-NDR system to exhibit periodic current oscillations. Details on this issue can be found in several comprehensive reviews and related articles (Koper, 1996b; Krischer, 1999; Krischer, 2003b).

As was mentioned above, on the basis of certain essential dynamical features, the Fe|H_2SO_4 system can be classified in the N-NDR category (Sazou et al., 1993a) where most of the metal|electrolyte systems belong. Therefore, only potentiostatic current oscillations are anticipated within a fixed potential region (Fig. 1b), when the IR_s exceeds an upper critical value, $IR_s > (IR_s)_{crit}$ bistability is expected, without oscillations. Under current-controlled conditions oscillations are not anticipated but only bistable behavior (Fig. 1d). The halide-perturbed Fe|H_2SO_4 system cannot be readily classified in one of the above categories and there is not doubt that it deserves a further investigation within this context. However, its dynamical behavior observed at relatively low chloride concentrations bears resemblance with the essential features of the HN-NDR oscillators (Krischer, 2003b). It seems, that oxide growth causes the NDR, whereas the slower action of chlorides on the oxide film and the gradual increase of passive-state current inhibits the appearance of NDR (Sazou et al., 2009).

4. Electrochemical behavior of the Fe|H_2SO_4 system

Fig. 3a illustrates the anodic current-potential (*I-E)* polarization curve of the Fe|0.75 M H_2SO_4 system traced under potential-controlled conditions at $\mathrm{d}E/\mathrm{d}t$=2 mV s^{-1} during both the forward and reverse backward potential scans. It seems that a variety of physico-

electrochemical processes occur upon increasing/decreasing the potential within the region between -0.5 – 2.5 V.

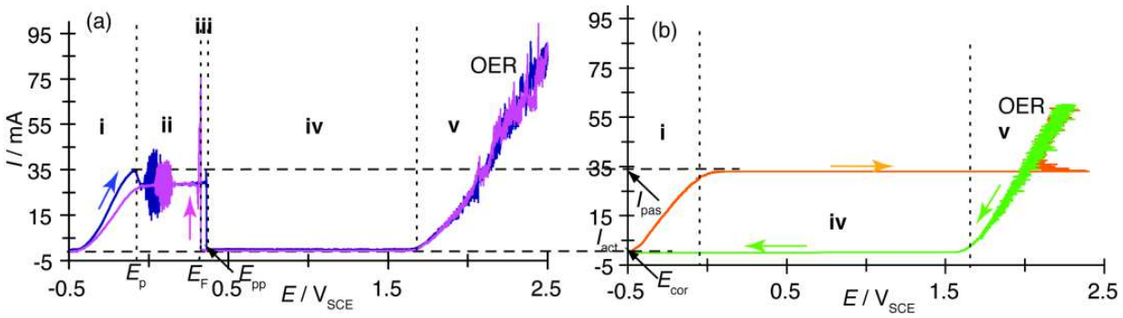

Fig. 3. (a) Potentiodynamic $I = f(E)$ curve traced at $dE/dt = 2$ mV s^{-1} and (b) galvanodynamic $E = f(I)$ curve traced at $dI/dt = 0.05$ mA s^{-1} of the Fe | 0.75 M H_2SO_4.

As can be seen in Fig. 3a, five typical regions are distinguished in the potentiodynamic *I-E* curve:

i. Active electrodissolution region, where Fe dissolution occurs from a film-free Fe surface through multiple stages (Keddam et al., 1984) and an overall reaction ,

$$Fe + nH_2O \rightarrow [Fe(H_2O)]^{2+} + 2e \quad (I)$$

ii. Limiting current region (LCR) where, under proper conditions, current oscillations may occur (Geraldo et al., 1998; Kiss et al., 2006; Kleinke, 1995; Sazou et al., 2000b; Sazou et al., 2000c; Sazou & Pagitsas, 2006b) beyond the peak potential, E_p and before the establishment of a steady transport-controlled LCR within which formation-dissolution of the ferrous salt, $FeSO_4.7H_2O$ proceeds at equal rates, according to the overall reaction,

$$Fe^{2+} + SO_4^{2-} + 7H_2O \leftrightarrow FeSO_4{\cdot}7H_2O \quad (II)$$

iii. Active-to-passive transition region, as defined during the forward potential scan (or passive-to-active transition region defined during the backward scan), associated with a hysteresis loop since transition to passivity, during the forward potential scan, occurs at the primary passivation potential, E_{pp} whereas reactivation of the Fe, during the backward scan, occurs at the Flade potential, E_F (Rush & Newman, 1995). The E_F and not the E_{pp} is considered as the passivation potential of the Fe electrode since the ohmic potential drop, IR_s becomes almost zero at E_F due to the very low current value established in the passive state traced during the backward scan. Therefore, the E_F determined in $I = f(E)$ curves is very close to the electrode potential V, which is related to the applied potential, E via the relationship, $E = V + IR_s$. In practice, R_s includes any series resistance added to the general EC of the electrochemical cell (Fig. 1e).

iv. The passive region, located between the E_F and transpassivation potential, E_{tr}. Transition of Fe to passivity can be represented by the overall reaction ,

$$Fe + x/2H_2O \rightarrow FeO_{x/2} + xH^+ + xe \quad (III)$$

v. The transpassive region, extended beyond the E_{tr}, where the oxygen evolution reaction (OER) occurs (Sazou et al., 2009).

The galvanodynamic *I-E* curve of the Fe|0.75 M H_2SO_4 system (Fig. 3b) differs from the corresponding potentiodynamic *I-E* curve (Fig. 3a) in that region **ii** is not recorded. A sudden transition to passivity and, in turn, to OER (region **v**) occurs during the forward current scan, while the LCR (region **iii**) is skipped. It seems that the sudden active-to-passive transition occurs once the ferrous salt layer is established at the critical current value, I_{pas}. The I_{pas} corresponds to the peak potential E_p of the potentiodynamic curve (Fig. 3a). During the backward current scan, Fe sustains passivity (region **iv**) up to the corrosion potential, E_{cor} whereas the passive-to-active transition occurs at a very low current, I_{act}. A hysteresis loop exists because $I_{pas} \neq I_{act}$. Potential oscillations are never observed under galvanostatic conditions at any applied current value up to 60 mA (Sazou et al., 2011; Sazou et al., 2009), in line with the galvanodynamic curve (Fig. 3b).

On the contrary, periodic current oscillations occur under potentiostatic conditions, immediately after switching on the potential within the oscillatory region, ΔE_{osc} at $E < E_F$ (ΔE_{osc} = 30-35 mV for the Fe|0.75 M H_2SO_4 system). Typical potentiostatic current oscillations occurring within the ΔE_{osc} are illustrated in Figs. 4a-c.

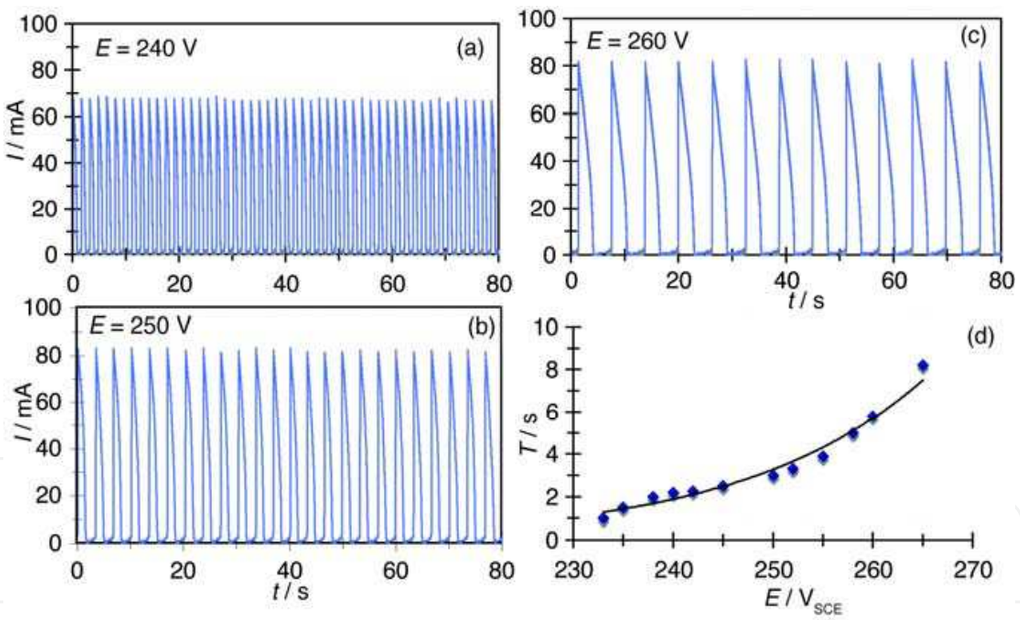

Fig. 4. (a-c) Potentiostatic current oscillations traced at different values of the applied potential, *E* and (d) dependence of the oscillation period, *T* on *E* for the Fe|0.75 M H_2SO_4 system.

Single periodic relaxation oscillations are revealed with a potential-dependent period, *T*. Fig. 4d shows that *T* increases upon increasing the potential (Podesta et al., 1979; Sazou et al., 1993a; Sazou & Pagitsas, 2003b). This indicates that the stability of the passive oxide film increases upon increasing the potential as a result of the increase of the oxide-film thickness and the concentration of Fe^{3+} in the oxide lattice (Engell, 1977; Vetter, 1971). The composition of the iron oxide film is related to Fe_3O_4 and γ-Fe_2O_3 (Toney et al., 1997) and its

stability is determined roughly by the ratio c_{Fe3+} / c_{Fe2+}. Increasing the $c_{Fe^{3+}}/c_{Fe^{2+}}$ ratio within the oxide film results in an increase of the oxide stability in acid media (Engell, 1977). Thus upon increasing the potential at $E > E_F$, the oxide structure is related rather with the stable γ-Fe_2O_3 than with the less stable in acidic solutions Fe_3O_4 prevailing at $E < E_F$ where oscillations may occur.

The mechanism of spontaneous current oscillations of the Fe|0.75 M H_2SO_4 system is understood on the basis of the early suggested Franck-FitzHugh (F-F) model (Franck, 1978; Franck & Fitzhugh, 1961) according to which periodic passivation/activation of the Fe occurs due to local *pH* changes (Rush & Newman, 1995; Wang & Chen, 1998) that lead to a shift of the E_F with respect to the electrode potential, *V* because the E_F depends on the *pH*,

$$E_F = 0.58\text{-}0.058pH \text{ vs. NHE at 293 K} \quad (3)$$

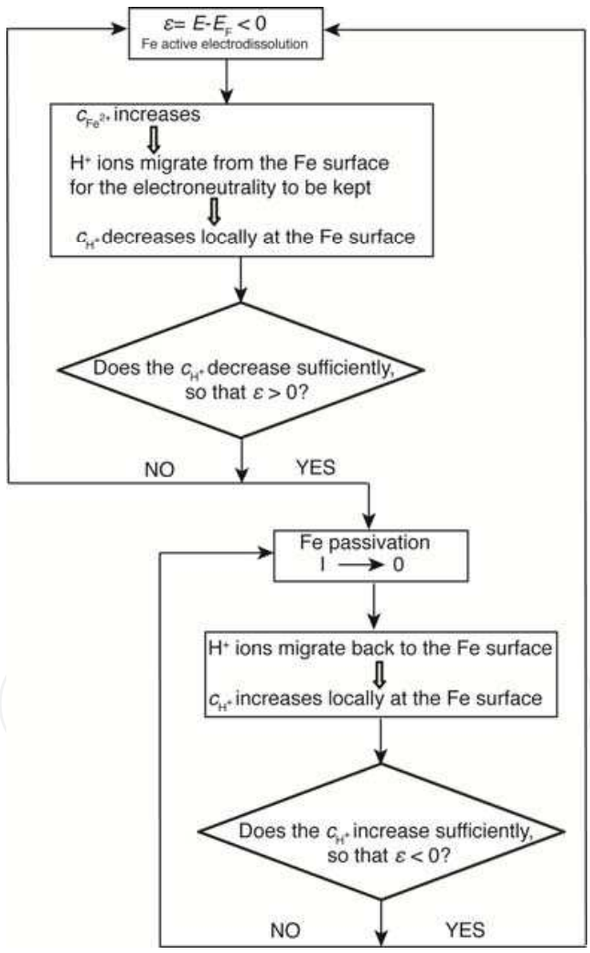

Fig. 5. Flow diagram illustrating the principle physico-electrochemcial processes involved in a current oscillatory cycle of the Fe|0.75 M H_2SO_4 system.

Furthermore, the formation of the ferrous salt layer and the ohmic potential drop, IR_s should be also taken into account for a realistic description of the periodic oscillations arisen across

the passive-to-active transition of Fe in acid solutions (Birzu et al., 2001; Birzu et al., 2000; Koper & Sluyters, 1993a; Pagitsas & Sazou, 1991; Rush & Newman, 1995). As was mentioned above, the electrode potential, V coincides with the applied potential, E at E_F. Therefore, $E - E_F = \varepsilon$ denotes the difference from the passivation potential. It becomes evident that at $\varepsilon < 0$, the Fe active electrodissolution via the overall reaction (I) occurs. Inversely, at $\varepsilon > 0$, passivation of the Fe via the overall reaction (II) occurs. In between, the LCR is esrablished through the reaction (III) (Pagitsas et al., 2003). These processes, identified in the $I = f(E)$ of the Fe|0.75 M H_2SO_4 system (Fig. 3), are in practice the principle physico-electrochemical processes occurring during an oscillation cycle. Identical processes are also taken into account in improved versions of the F-F model (Koper & Sluyters, 1993a; Krischer, 2003a) as can be seen in the flow diagram displayed in Fig. 5.

5. Chemical perturbation of the Fe|H_2SO_4 system by adding small amounts of halides

In a series of studies, was shown that addition of halides, X ≡Cl^-, Br^-, I^- gives rise to changes in both the potentiodynamic I=f(E) (Pagitsas & Sazou, 1999; Sazou et al., 2000a; Sazou et al., 2000b; Sazou & Pagitsas, 2003b; Sazou et al., 1993b; Sazou et al., 1992; Sazou et al., 2009) and galvanodynamic E = f(I) curves (Sazou et al., 2011; Sazou et al., 2009) of the Fe|0.75 M H_2SO_4 system. All halide-induced changes can be identified approximately within regions **i-v** (Fig. 3). This indicates that halides participate in both the electrodissolution and passivation processes of Fe. However, since this article focuses on features that might be exploited to characterize pitting corrosion, special emphasis is placed on the passive and passive-active transition states of Fe.

The halide-induced changes together with nonilinear phenomena are investigated first on the basis of potentiodynamic, I = f(E) and galvanodynamic, E = f(I) curves. These curves can be considered as characteristic curves of the nonlinear system under study, in an analogy with the semiconductor "characteristic curve" used in solid state physics, or as a one-parameter "phase diagram" or "bifurcation diagram" in terms of nonlinear dynamics. Characteristic I = f(E) and E = f(I) curves exhibit all transitions between different steady and oscillatory states upon varying the applied potential acting as a bifurcation parameter. Then, the different states of the system being known, current or potential time-series are recorded under potentiostatic or galvanostatic conditions, respectively, at potentials or current values located within the corresponding oscillatory regions. A slight deviation is noticed in determining the upper and lower limits of the oscillatory region under static conditions as compared with dynamic I = f(E) and E = f(I) curves.

5.1 Under potential-controlled conditions

The effect of an increasing chloride concentration, within a relatively low-concentration range ($c_{Cl^-} < 20$ mM), on potentiodynamic I= f(E) curves is displayed in Fig. 6.

Inspection of the I= f(E) curves of Fig. 6, reveal that pitting corrosion manifests itself in changes that are summarized as follows:

1. The halide-induced oscillatory region, $\Delta E_{osc,Cl}$, relative to the halide-free ΔE_{osc}, is extended towards higher potentials ($\Delta E_{osc,\,Cl} > \Delta E_{osc}$).

2. The lower, E_{low} and upper, E_{upp} potential limits of the oscillatory region shift towards higher values indicating destabilization of the stable passive state existing in the halide-free system. It is found that both E_{low} and E_{upp} vary linearly with the log(c_{Cl}-). Appropriate analysis, leads to the critical values of c_{Cl}-, beyond which oxide formation becomes unlikely and hence transition to a mass-transport LCR may occur due to the formation-dissolution of ferrous salts signifying a stable pit growth. This value is found to be ~30 mM in agreement with experimental observations (Sazou et al., 2000a; Sazou et al., 2000b).
3. The current in the passive state increases. It is lower during the forward potential scan ($I_{pas,f}$ in Fig. 6b) than during the backward one ($I_{pas,b}$ in Fig. 6c). This can be interpreted considering that pitting corrosion is a dynamical process and therefore, the longer time elapsed for the backward scan allows the progress of pit propagation and/or growth to a greater degree than during the forward scan.
4. The maximum oscillatory current, $(I_{osc})_{max}$ (Fig. 6b) deviates from the kinetics of the linear segment in region **i**, indicating a larger real surface of the Fe electrode. This is attributed to the increase of the surface roughness due to pitting corrosion as compared with the uniformly corroding Fe surface in the halide-free system (Fig. 6a). The magnitude of the deviation is expressed as the ratio $(I_{osc})_{max}/(I_{osc})_{max,\ exp}$, where the $(I_{osc})_{max,\ exp}$ is the current expected on the basis of the relationship $E = V + IR_s$. The latter relationship is valid in the linear segment of the active region **i** located beyond the Tafel region (Pagitsas et al., 2007; Pagitsas et al., 2008).
5. No access to E_{tr} is possible whereas the critical pitting potential E_{pit} appears (Fig. 6b). The E_{pit} is the critical potential for stable pitting to occur.

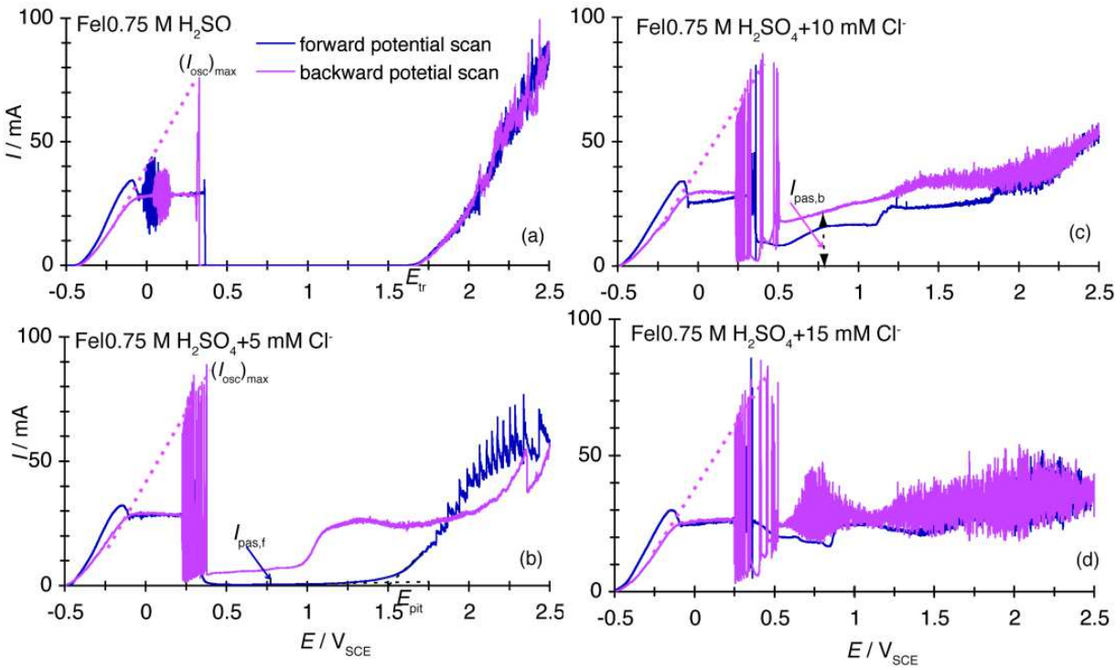

Fig. 6. Chloride-induced changes in the potentiodynamic I= f(E) curves of the Fe|0.75 M H_2SO_4 system traced at dE/dt = 2 mV s^{-1}.

Moreover, Fig. 6 shows that increasing gradually the c_{Cl^-} the current in the passive state increases (Table 1). At c_{Cl^-} > 15 mM, both $I_{pas,f}$ and $I_{pas,b}$ tend to reach a limiting value within the potential region between ~0.3 and 2.5 V whereas new oscillatory states emerge out of the passive state. These current oscillations are associated with the precipitation-dissolution of ferrous salt layers in front of pits grown on the Fe surface, while the OER rate diminishes (Sazou et al., 2000b; Sazou & Pagitsas, 2003a).

Adding Br^- and I^- ions leads to similar changes in the corresponding potentiodynamic *I-E* curves with those mentioned above. However, comparing quantities such as the $(I_{osc})_{max}/(I_{osc})_{max,\,exp}$, ΔE_{osc} and the current in the passive state allows characterization of the extent of pitting corrosion induced by each halide ion (Sazou et al., 2000a). This becomes obvious from Table 1, which summarizes the values of these quantities for all halides in comparison with those obtained for the halide-free Fe|0.75 M H_2SO_4 system. At relatively low halide concentrations, these quantities depend on c_{X^-} and the aggressiveness of halides. It is thus concerned with localized oxide breakdown and repeated activation-repassivation events of the entire Fe-disc surface at early stages of pitting corrosion. However, depending on the halide identity, additional individual differences are noticed in the case of I^- and fluoride species. In the former case, it is observed that $I_{pas,f} > I_{pas,b}$, which is an inverse relationship compared to that anticipated for pitting corrosion induced by Cl^- and Br^-. This is assigned to the formation of a compact iodine layer over the Fe surface due to iodide electrochemical oxidation. Iodine layer seems to prevent the evolution of pit growth. In he case of fluoride species, though the ΔE_{osc} is extended towards higher potentials, drastic changes in the $I_{osc,\,max}$ and the current in the passive state are not observed indicating an enhanced general corrosion instead of pitting.

Addition	c (mM)	ΔE_{osc} (mV)	$I_{pas,\,f}$(mA)	$I_{pas,\,b}$(mA)	$(I_{osc})_{max}/(I_{osc})_{max,\,exp}$	E_{tr} , E_{pit} (V)
None	-	235-270	0.15	0.15	1.01	1.65
NaF	10	240-290	0.22	0.22	1.05	1.65
	20	245-310	0.25	0.25	1.03	1.65
NaCl	10	240-380	2.4	13.7	1.2	1.00
	20	290-520	23.7	22.4	1.23	LCR
NaBr	10	255-500	3.9	3.7	1.13	1.4
	20	280-700	22.5	22.5	1.18	LCR
NaI	10	243-440	6.8	1.12	1.01	1.55
	20	245-450	5.5	0.6	1.02	1.37

Table 1. Effect of halide ions, X^- on the oscillatory potential region ΔE_{osc}, the current in the passive state observed during the forward, $I_{pas,f}$ and backward, $I_{pas,b}$ potential scans, the maximum oscillatory current ratio $(I_{osc})_{max}/(I_{osc})_{max,\,exp}$ and the transpassivation potential, E_{tr} or the pitting potential, E_{pit} appeared in the presence of X^-.

Besides changes observed in potentiodynamic $I = f(E)$ curves, pitting corrosion manifests itself in potentiostatic current oscillations too. An example of halide-induced oscillations is given in Fig. 7a. Fig. 7a displays a transition between single periodic oscillations observed in the halide-free system, immediately after switching on the potential at $E < E_F$, and the halide-induced complex periodic oscillations appeared after an induction period of time, t_{ind} (Fig. 7b). The halide-induced current oscillations occur over a wide potential region (Table 1) and their periodicity was found to follow period doubling, quadrupling and aperiodicity by increasing the applied potential, E and c_{X^-} (Sazou et al., 2000b). Depending on E and c_{X^-} different temporal patterns were recorded such as bursting and beating. Variation of the current waveform was also observed at longer times as it is anticipated for pitting corrosion, being strongly- dependent on time (Sazou et al., 2000b; Sazou et al., 1993b).

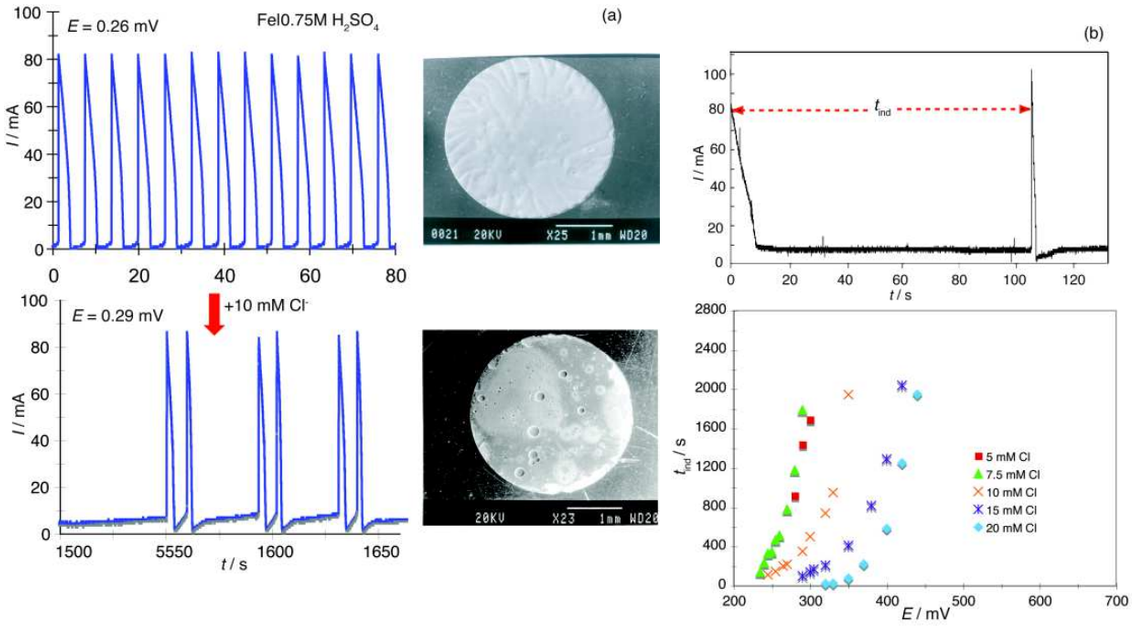

Fig. 7. (a) Transition of the single periodic to a complex periodic current oscillation induced by adding Cl^- into the Fe|0.75 M H_2SO_4 system. Next to each oscillation waveform, SEM micrographs display the corresponding Fe surface morphologies. (b) Induction time, t_{ind} occurring prior the onset of chloride-induced oscillations and dependence of t_{ind} on the potential at various c_{Cl^-}

The complex oscillations induced by Cl^- as well as Br^- and I^- is the result of the aggressive action of halides on the Fe surface (Sazou et al., 2000a; Sazou et al., 2000b). This is confirmed by SEM observations, an example of which is depicted in Fig. 7a. The morphology of the Fe-disc surface during the occurrence of single periodic oscillations reflects a general corrosion induced by H^+ ions. Hydrogen ions catalyze the uniform dissolution of the passive oxide film consisting primarily of Fe_3O_4 (Engell, 1977; Sato, 1990). Associated with temporal current patterning, are also spatial phenomena that deserve to be investigated (Hudson et al., 1993). On the other hand, when complex periodic current oscillations occur in the presence of chlorides and other X^- ions, the morphology of the Fe surface reveals hemispherical pits as a result of the local breakdown of passivity on Fe. Local active areas

generated by the local action of halides results in an inhomogeneous passive Fe surface and perhaps in new spatiotemporal patterns.

It is noted that besides the potential, the solution resistance, R_s or equally a variable external series-resistance, R_{ex} inserted between the working and reference electrodes, the rotation speed, ω of the rotating Fe-disc electrode, the solution *pH* and temperature, all parameters control the nonlinear behavior of the Fe|0.75 M H_2SO_4 electrochemical oscillator. However, though these contol parameters influence the onset, the period and amplitude of oscillations, none of them changes the oscillation waveform. Whenever current oscillations appear across the passive-to-active transition region (at $E < E_F$), they are single periodic of relaxation type. To our knowledge, the type of these oscillations will change only when a halide-induced chemical perturbation of the passive state of the Fe| H_2SO_4 system is conducted and pitting instead of uniform corrosion occurs. This is a striking indication that new physico-electrochemical processes have been triggered by halides manifested in the variety of complex oscillations.

Inspection of Fig. 7b shows that a fluctuating steady current exist during the induction period of time, t_{ind} elapsed before the onset of oscillations. This is indicative of the aggressive action of Cl^-, which leads to the nucleation of small pits that in turn are repassivated immediately. It proceeds until a complete destabilization of the passive state occurs (1st activation event). The transition to the active state is followed by repeated passivation-activation events (complex oscillations) that constitute a phenomenon termed as unstable pitting corrosion. Therefore, the t_{ind} characterizes the kinetics of the oxide attack by X^- ions. It was found that t_{ind} depends on both the c_{X^-} and *E*. An example is given in Fig. 7b for a chloride- perturbed Fe|0.75 M H_2SO_4 system. As Fig. 7b shows, increasing the c_{X^-} leads to the decrease of t_{ind} indicating promotion of the local breakdown of the oxide film. On the contrary, increasing the applied potential the t_{ind} increases. The rate of unstable pitting corrosion diminishes by increasing the potential due to the enhancement of oxide stability.

Another quantity describing quantitatively the competitive process between halide action and enhancement of oxide stability is the oscillation period, *T*. As can be seen in Fig. 8a, *T* decreases with c_{Cl^-}, while it increases with *E*. It is noticed that the increase of *T* observed at lower c_{Cl^-} is interpreted in terms of changes in periodicity since period doubling and quadrupling occurs. More accurate empirical relationships are obtained if an average activation rate (number of spikes over a period of time) is employed instead of *T* (Pagitsas et al., 2001; Pagitsas et al., 2002; Sazou et al., 2000a).

In this context, it should be noted that the decrease of *T* with c_{Cl^-} is also associated with the general corrosion occurring concurrently with unstable pitting corrosion. As can be seen in Fig. 8b, a similar dependence of *T* on the concentration of fluoride species is also obtained. It is well known that fluorides in acid solutions (*pH* ~ 0-0.5) cause general corrosion but not pitting since HF is the largely predominant species, while other fluoride species may coexist at negligible amounts (Pagitsas et al., 2001; Pagitsas et al., 2002; Strehblow, 1995). In agreement with the fluoride effect, is also the effect of c_{H^+} on *T* (Sazou & Pagitsas, 2003b). As was mentioned above, the onset of current oscillations in the halide-free Fe|0.75 M H_2SO_4 system is assigned to destabilization of the oxide film due to *pH* changes occurring uniformly at the Fe surface (Eq. (3)). In this case, general corrosion of the oxide film is

induced by H^+ ions only around the E_F (Fig. 3) and hence T decreases with increasing the c_{H+} (Sazou & Pagitsas, 2003).

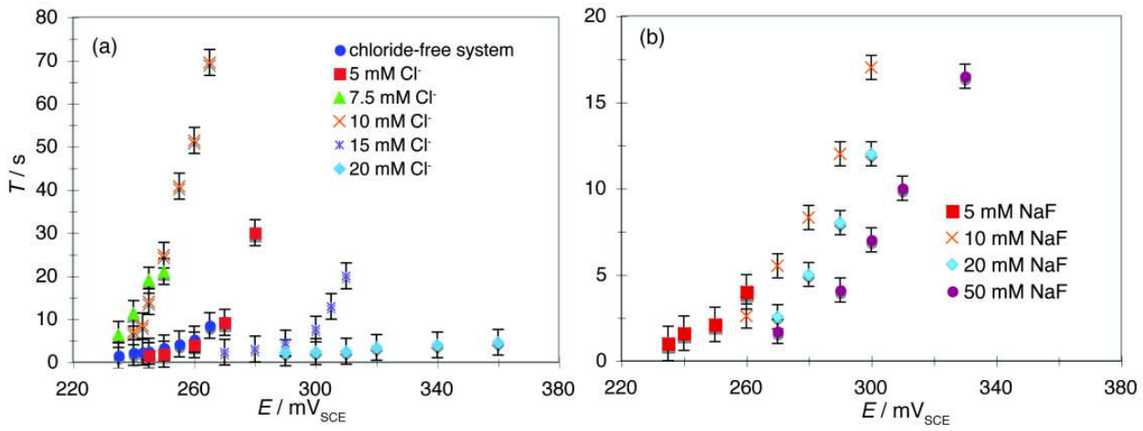

Fig. 8. Dependence of the oscillation period, T as a function of the applied potential, E at (a) various c_{Cl^-} and (b) various concentrations of fluoride species.

Therefore, distinction between pitting and general corrosion is possible on the basis of quantities obtained from both potentiodynamic $I = f(E)$ and potentiostatic $I = f(t)$ curves. Besides, Cl^-, Br^-, I^- and fluoride species, chlorates and perchlorates were also used in perturbing the Fe|0.75 M H_2SO_4 system (Pagitsas et al., 2007; Pagitsas et al., 2008). The effect of chlorates and perchlorates on the Fe passive surface, being disputable in the literature, was clarified using all the above-mentioned diagnostic criteria including ΔE_{osc}, $I_{pas,f}$ and $I_{pas,b}$, $(I_{osc})_{max}/(I_{osc})_{max,\,exp}$, E_{pit}, t_{ind} and T.

Moreover, these diagnostic criteria were also tested in the presence of nitrates in chloride-containing sulfuric acid solutions (Sazou & Pagitsas, 2002). Newman and Ajjawi characterized the effect of nitrates on stainless steel as peculiar (Newmann & Ajjawi, 1986). Regarding pitting corrosion, nitrates may act either as activating or inhibiting species (Fujioka et al., 1996). This property of nitrates was also realized in the case of Fe. It is manifested in several features of current oscillations observed over a wide potential region. Appropriate analysis of $I = f(E)$ and $I = f(t)$ curves demonstrated that nitrates may stimulate pitting corrosion at lower potentials, while may cause a sudden passivation of Fe at higher potentials. This behavior is interpreted by taking into account the electrochemical and homogeneous chemical reactions of nitrates. Current oscillation seems to be a suitable probe to indicate both qualitatively and quantitatively if a stable passive state is established in corrosive media (Sazou & Pagitsas, 2002).

5.2 Under current-controlled conditions

Fig. 9 shows galvanodynamic $E = f(I)$ curves of the Fe|0.75 M H_2SO_4 system traced at gradually increasing c_{Cl^-}. Chlorides seem to induce:

1. Potential oscillations at a critical c_{Cl^-}.
2. Occurrence of more potential oscillations during the backward current scan as well as by increasing c_{Cl^-}.

3. Considerable increase of I_{act} with a slight decrease of I_{pas} by increasing c_{Cl^-}. Hence the width of the hysteresis loop, $\Delta I = |I_{pas} - I_{act}|$ decreases (Fig. 9a). The I_{pas} and I_{act} are defined as the critical current values where transition to passive and active states occurs during the forward and inversely backward current scans, respectively.

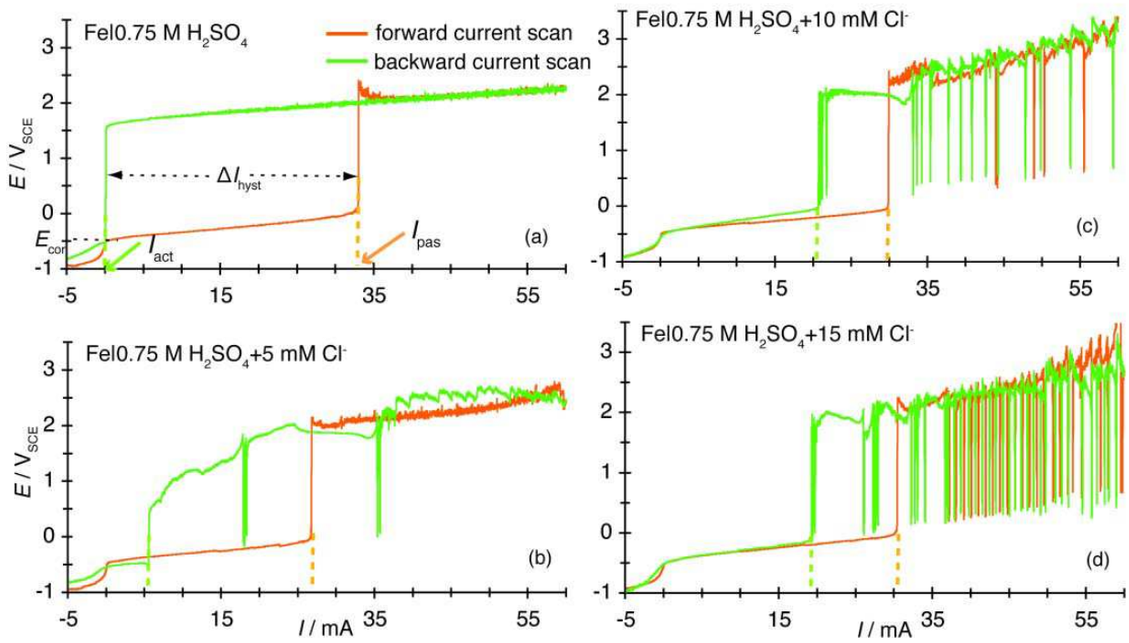

Fig. 9. Chloride-induced changes in the galvanodynamic $E = f(I)$ curves of the Fe|0.75 M H_2SO_4 system traced at $dI/dt = 0.05$ mA s^{-1}.

Apparently, potential oscillations in galvanodynamic $E = f(I)$ curves constitute manifestation of pitting corrosion since, as was mentioned in sections 3 & 4, no oscillations should occur for the halide-free Fe|0.75 M H_2SO_4 system under a current control. Corresponding changes in $E = f(I)$ curves are also induced by adding other halide species. An example of $E = f(I)$ curves at 20 mM of fluorides, Cl^- , Br^- and I^- ions is illustrated in Fig. 10.

Comparing the $E = f(I)$ curves illustrated in Fig. 10, it seems that fluorides do not induce potential oscillations, as it should be anticipated, since fluorides cause only general corrosion of the Fe surface. In the present case, general corrosion proceeds concurrently with the OER exemplifying itself by the occurrence of small amplitude potential fluctuations due to the formation and subsequent escape of oxygen bubbles from the Fe surface (Fig. 10a). Regarding Br^-, potential oscillation does appear (Fig. 10c), though to a lesser degree than in the presence of Cl^- (Fig. 10b), in agreement with the lesser aggressiveness of Br^- as compared with that of Cl^-.

Inspecting Fig. 10d, one may see that no pitting corrosion occurs in the presence of I^-. However, it is well known that iodide does cause pitting corrosion (Strehblow, 1995), manifested also in both the $I=f(E)$ and $I=f(t)$ curves (Pagitsas et al., 2002; Sazou et al., 2000a). This apparent discrepancy can be interpreted by taking into account oxidation processes of iodides that result in the formation of a solid iodine film on the Fe surface (Ma & Vitt, 1999;

Vitt & Johnson, 1992). This iodine film hinders the activation of the Fe surface expected to occur due to the localized action of I^-. Thus any noticeable increase of I_{act} is not shown. In fact, the I_{act} remains equal with that of the unperturbed system (Fig. 9a). Instead of large amplitude oscillations, indicative of localized corrosion, a new type of potential oscillation emerges (Fig. 10d) associated with the OER occurring concurrently with the formation-dissolution of the iodine layer. The features of these low amplitude oscillations are influenced by the c_{I^-} and applied current values and become more pronounced at higher c_{I^-} (~50 mM). Therefore, the electrochemical and chemical behavior of I^- together with their action on the passive Fe surface becomes very complicated under current-controlled conditions. Further investigation within a different context deserves to be carried out.

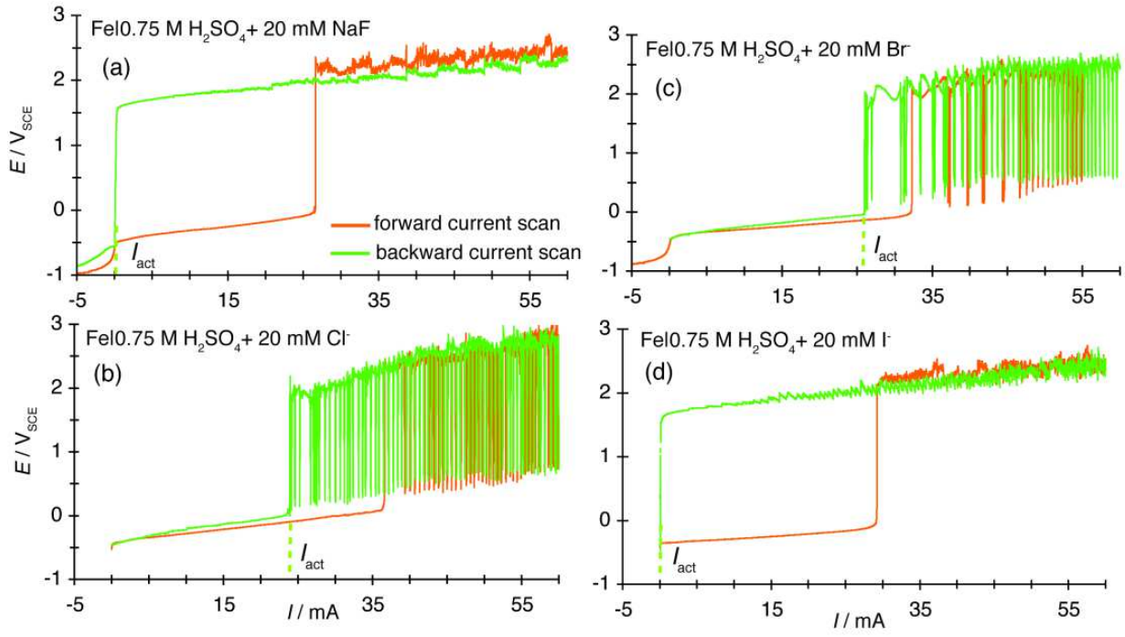

Fig. 10. Comparison of the effect of various halide species on the galvanodynamic $E = f(I)$ curves of the Fe | 0.75 M H_2SO_4 system traced at $dI/dt = 0.05$ mA s^{-1}.

Table 2 summarizes the values of I_{pas} and I_{act} obtained for the halide-free Fe | 0.75 M H_2SO_4 system in comparison with the corresponding values evaluated for the halide-perturbed one. The occurrence of potential oscillations and the quantity I_{act} are associated with pitting corrosion. The I_{act} increases by increasing either the halide concentration or the aggressiveness of halides implying stimulation of pitting corrosion. The higher the I_{act} or the lower the width of the hysteresis loop is, ΔI, the greater is the susceptibility of Fe to pitting corrosion. Comparing the aggressiveness of Cl^- and Br^- in terms of the I_{act} or ΔI , the order Cl^- > Br^- is found, in agreement with the order found from the nonlinear dynamical response obtained under potential-controlled conditions (Pagitsas et al., 2002; Sazou et al., 2000a), as well as with literature data based on other criteria (Janik-Czachor, 1981; Macdonald, 1992; Strehblow, 1995).

The current region within which potential oscillations are expected to occur at a constant applied current, I_{appl} can be deduced from the E=f(I) curves. As was mentioned in the

beginning of this section, E=f(I) curves represent roughly one-parameter bifurcation diagrams. It seems that, for oscillations to occur, the I_{appl} should be approximately higher than I_{act}. Fig. 11 shows examples of galvanostatic E=f(t) curves traced for 20 min at I_{appl} = 30 mA for the halide-free and chloride-perturbed Fe | 0.75 M H_2SO_4 system at different c_{Cl^-}.

Addition	c (mM)	I_{pas} (mA)	I_{act} (mA)	$\Delta I = I_{pas} - I_{act}$
None	-	33	0.15	32.85
NaF	10	33	0.22	32.78
	20	32	0.25	31.75
NaCl	10	30	20	10
	20	29	25	4
NaBr	10	32	18	14
	20	29	22.6	6.4
NaI	10	24	0.15	23.85
	20	28.9	0.15	28.75

Table 2. Effect of halides, X^- on the current, I_{pas} at which transition to passivity occurs during the forward current scan, the current I_{act}, where reactivation occurs during the backward current scan and the width of the hysteresis loop, ΔI defined from galvanodynamic curves (dI/dt=0.05 mA s^{-1}) of the Fe | 0.75 M H_2SO_4 system.

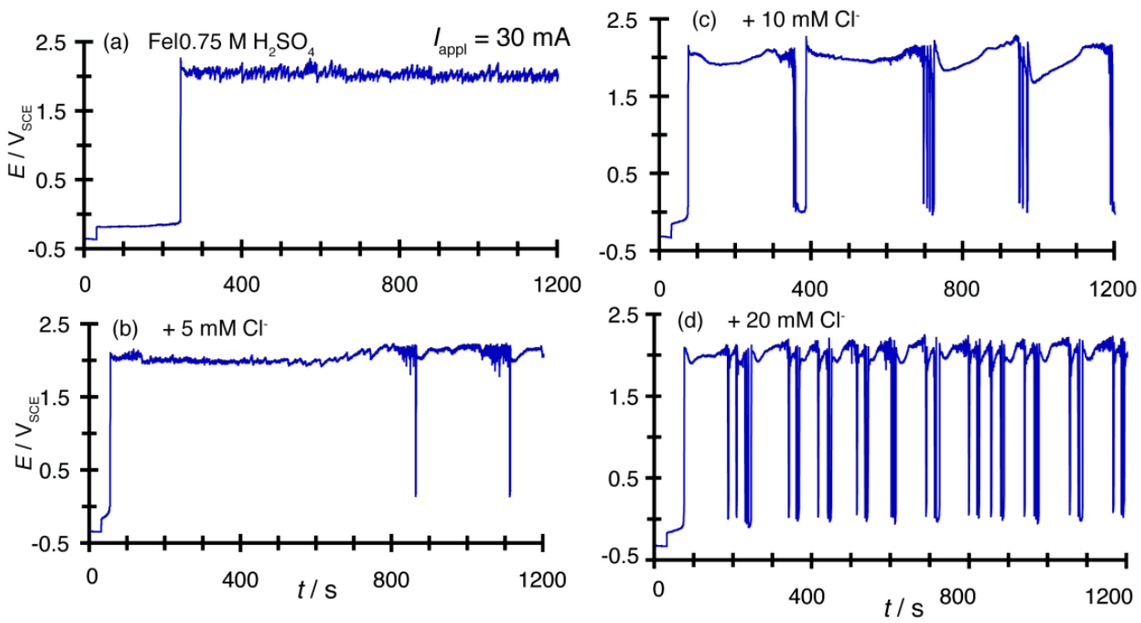

Fig. 11. Chloride-induced potential oscillations of the Fe | 0.75 M H_2SO_4 system traced under galvanostatic conditions at I_{appl}=30 mA.

Similar potential oscillations, with those illustrated in Fig. 11, were also observed in the presence of Br^-. In summary, chloride- and bromide-induced changes in galvanostatic E=f(t) curves at constant I_{appl} for various c_{Cl^-} and at constant c_{Cl^-} for various I_{appl} include:

1. Onset of potential oscillations of large amplitude (~2 V) when c_{Cl^-} is higher than a critical value (>5 mM) and only if $I_{appl} > I_{act}$.
2. The potential oscillates between the two steady states, namely the passive and active states. This indicates that initiation of pitting results in the destabilization of passivity on Fe and activation of the entire Fe surface.
3. Different waveforms of potential oscillations depending on c_{Cl^-} (or c_{Br^-}) and I_{appl} with an average frequency that increases with increasing c_{Cl^-} and I_{appl}.
4. Occurrence of certain induction period of time, t_{ind} before oscillations start, which decreases by increasing the c_{Cl^-} and I_{appl}.

The dependence of t_{ind} and average oscillation frequency with c_{Cl^-} and I_{appl} is displayed in Figs. 12a, b. The oscillation frequency is expressed as the average firing rate, <r> defined by the ratio, <r> = $N/\Delta\tau$, where N is the number of spikes (passive-active events) appeared during a fixed duration, $\Delta\tau$ of the experiment (Dayan & Abbott, 2001). The N is measured at $t > t_{ind}$ (Sazou et al., 2009). It becomes clear that t_{ind} reflects the kinetics of pit initiation on the passive Fe surface whereas <r> is rather related to the pit growth and propagation. Therefore, both t_{ind} and <r> can be used to describe quantitatively pitting corrosion on passive Fe. The quantities t_{ind} and <r> are currently used to estimate the inhibiting effect of nitrates on pitting corrosion.

When Fe is in the passive state (high-potential state) and chlorides start their action generating local active areas on the Fe surface, the oxide becomes gradually dark brown due to the conversion of its outer layer into ferrous oxo-chloride complexes. At the moment of Fe activation, all anodic layers, being separated from the Fe substrate, seem streaming away from the electrode. Due to the high current, the active Fe surface abruptly passivates and correspondingly the potential increases to its highest value. SEM images reveal an inhomogeneous growth of the passive oxide since it covers both localized activated and perhaps never-activated sites.

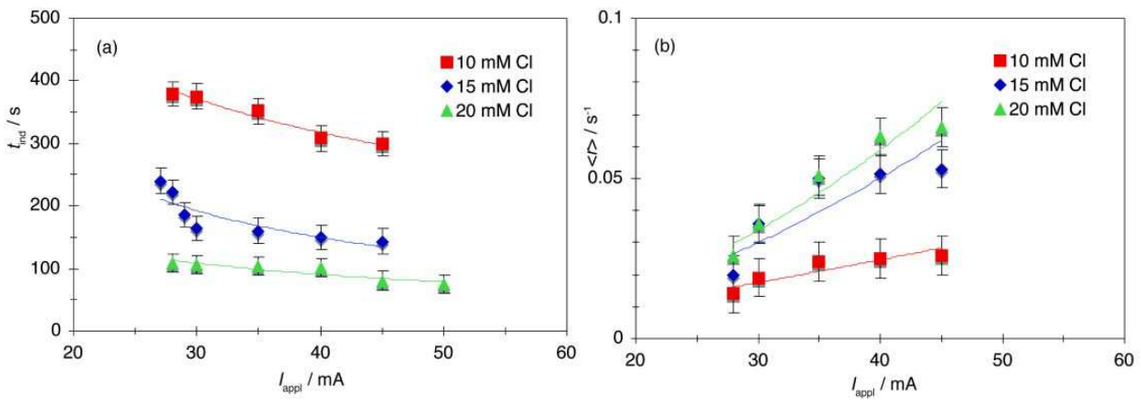

Fig. 12. Dependence of the (a) induction time, t_{ind} required for potential oscillations to start and (b) average firing rate, <r> as a function of the applied current, I_{appl} and c_{Cl^-} for the chloride-perturbed Fe | 0.75 M H_2SO_4 system.

The mechanism of passive-active oscillations associated with unstable pitting corrosion includes the formation and detachment of the oxide film that can be sufficiently explained in terms of the point defect model (PDM) (Macdonald, 1992; Pagitsas et al., 2001; Pagitsas et al., 2002; Pagitsas et al., 2003; Sazou et al., 2009). PDM is a realistic quantitative model that includes many of the oxide properties and explains many of the experimental observations during oxide growth and its breakdown. The processes leading to pitting corrosion are associated with the occupation of oxygen vacancies by halides, X^-. This reaction results in perturbation of a Schottky-pair equilibrium and autocatalytic generation of cation vacancies. Cation vacancies accumulate at the Fe|oxide interface leading to the formation of void and separation of the oxide from the Fe substrate. Simultaneously, the thickness of the oxide film decreases due to general corrosion through the formation of surface complexes between iron lattice-cations and halides. When the void exceeds a critical size and the oxide film over the void thins below a critical thickness film breakdown occurs at this particular site (Macdonald, 1992; Sazou et al., 2009).

At sufficiently high c_{Cl^-} or c_{Br^-}, dissolution rates are enhanced whereas oxide formation becomes unlikely. Instead, formation of ferrous salt layers is facilitated leading to the electropolishing dissolution state (Li et al., 1993; Li et al., 1990). This situation is discussed briefly below only in the case of potential-controlled conditions.

6. Non-linear dynamical response of the Fe|H_2SO_4 system at relatively high concentrations of halides

Fig. 13a shows that at relatively high halide concentrations (i.e. $c_{Cl^-} > 20$ mM), Fe cannot sustain passivity and a limiting current region (LCR) is established out of the passive state within 0.3 and 2.7 V (the upper potential limit used in the potentiodynamic measurements). This LCR is due to the precipitation-dissolution of salt layers since the oxide growth is prevented by Cl^- and differs from the LCR appeared for $E < E_F$, where oxide formation is thermodynamically prohibited. Within this "new" LCR, two distinct types of current oscillations are observed.

- Type I, called also as passive-active oscillations appeared within the lower potential regime ($E < 0.6$ V) either as a continuous spiking (beating) or aperiodic bursting. These oscillations arise out of a limiting current state with a full-developed amplitude and differ from those observed at relatively low c_{Cl^-} , which arise out of a passive state (Fig. 7).
- Type II, chaotic oscillations of a relatively small amplitude occurring at higher potentials ($E > 0.6$ V). The extent of each oscillatory regime depends on the halide concentration and halide identity. Upon a further increase of c_{Cl^-}, the regime corresponding to oscillations of type I is restricted gradually. For c_{Cl^-}>40 mM, current oscillations of type II dominate the entire LCR for $E > 0.3$ V (Fig. 13a).

An induction period of time, t_{ind} is elapsed before current oscillations of type I or II appear. During t_{ind}, the current reaches a steady state value during which precipitation-dissolution of ferrous salts occurs at equal rates. Precipitation of ferrous salt occurs inside pits when a local supersaturation condition for Fe^{2+} and sulfates/chlorides is reached. There are evidences (Sazou & Pagitsas, 2003a) that the bifurcation potential, E_{bif}, for the transition from oscillations of type II to those of type I coincides with the repassivation potential, E_R

used in pitting corrosion studies under steady state conditions (Sato, 1987; Sato, 1989). E_R it is the critical potential at which a transition from a polishing state dissolution (bright pits) to active state dissolution (etching pits) occurs. Critical conditions for the onset of different types of oscillations may be defined in terms of the critical pit solution composition (critical c_{Cl^-} and c_{H^+}) at which Fe cannot sustain passivity and, thereby, pit stabilization is possible (Sazou & Pagitsas, 2003a).

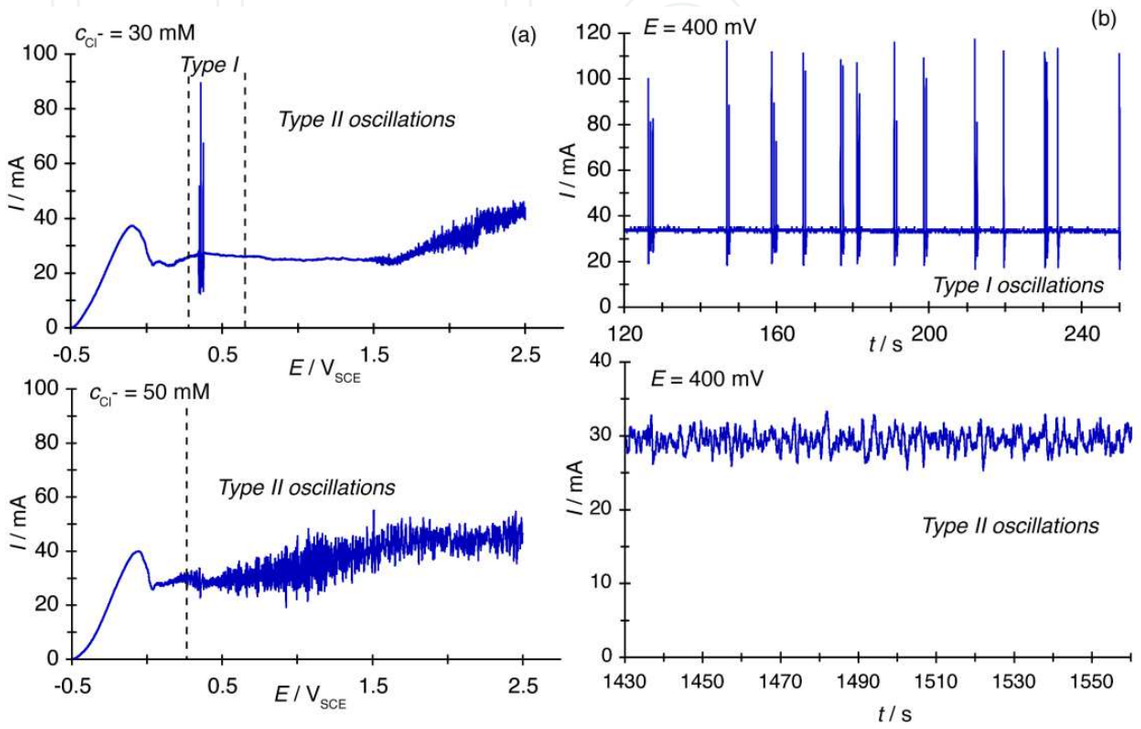

Fig. 13. (a) Non-linear dynamical response of the Fe|0.75 M H_2SO_4 system in the presence of relatively high c_{Cl^-}. It exhibits a transition from a situation where oscillations of type I and II appear in the *I*-*E* curves to one where oscillations of type II dominate the whole LCR at E > 0.3 V. Polarization curves were traced at dE/dt = 2 mV s^{-1}. (b) Representative examples of type I and type II current oscillations corresponding to the I=f(E) curves shown in (a).

An example of a potential-induced transition between potentiostatic current oscillations of type I (aperiodic bursting) to those of type II (low amplitude chaotic oscillations) is illustrated in Fig. 14 for the Fe|0.75 M H_2SO_4 + 30 mM Cl^- system. It seems that this transition occurs around E_{bif} = 0.55 V which coincides with the E_R (Sazou & Pagitsas, 2003a).

Oscillations of type II occurring at either high potentials of the oscillatory region at relatively low c_{Cl^-} or within the entire oscillatory region at sufficiently high c_{Cl^-} originate from processes similar to those responsible for chaotic oscillations observed at the beginning of the LCR (E < 0.3 V) shown in the I = f(E) curve of the halide-free Fe|0.75 M H_2SO_4 system (Fig. 3a) (Sazou & Pagitsas, 2006b). Supersaturation conditions of the ferrous salts established inside pits results in a density gradient Δd between the solution in the interfacial regime in front of the Fe electrode and the bulk solution. When Δd exceeds a critical value the steady limiting current becomes unstable. This condition is fulfilled in

the presence of a critical *IR* drop (Georgolios & Sazou, 1998; Pickering, 1989; Pickering & Frankenthal, 1972).

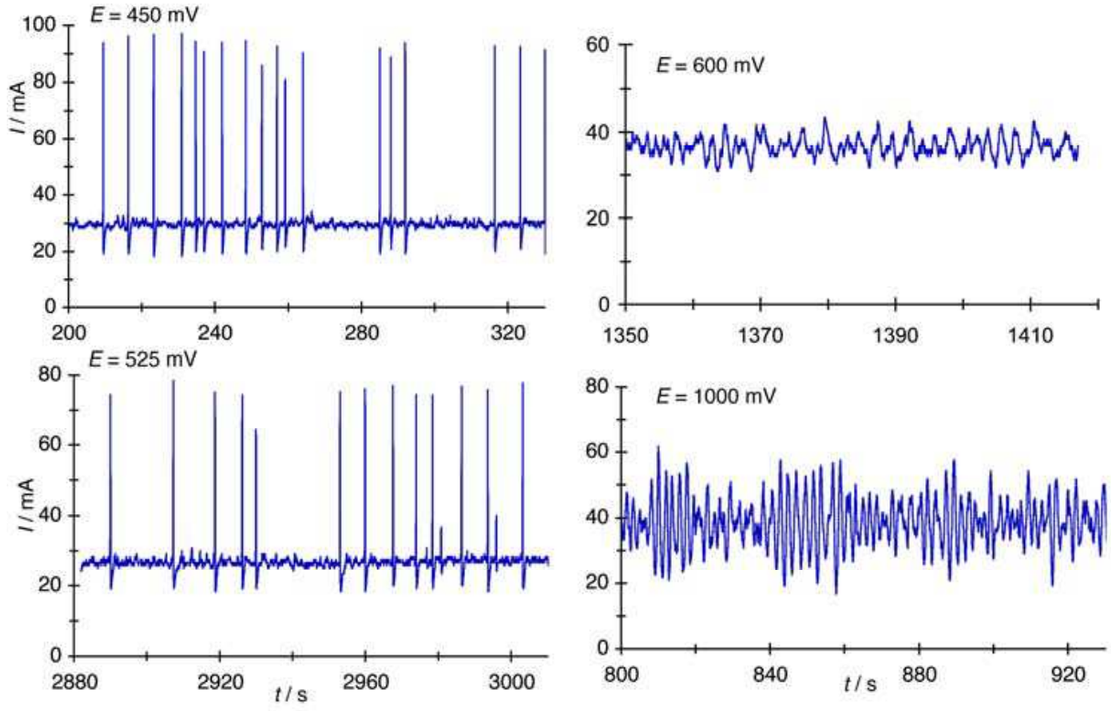

Fig. 14. Sequence of current oscillations at late stages of pitting corrosion of Fe in 0.75 M H_2SO_4 + 30 mM Cl^- displaying a transition from oscillations of type I to those of type II upon increasing the applied potential, *E*.

7. Alternate diagnostic criteria to characterize pitting corrosion at early stages of pitting corrosion

It becomes clear that the non-linear dynamical response of the halide-perturbed Fe|0.75 M H_2SO_4 system exemplified either under potential- or current-controlled conditions reflects the aggressive action of halide ions, especially of Cl^- on the Fe passive oxide film. Steady-state processes leading to passive and active states of Fe in a halide-free sulfuric acid solution are perturbed through a series of physico-electrochemical reactions including autocatalytic steps. In fact, pit nucleation, propagation and growth are autocatalytic processes (Budiansky et al., 2004; Lunt et al., 2002; Macdonald, 1992). Pit repassivation or stable growth can be realized by investigating the system oscillatory states and oscillation waveform. Therefore, oscillations might be used like a "spectroscopic" technique to detect pitting corrosion and moreover to characterize unstable and stable stages during pit evolution. A summary of oscillatory phenomena expected to arise at different stages of pitting corrosion can be seen in the flow diagram displayed in Fig. 15.

Under potential-controlled conditions, the nonlinear dynamical response of the halide-perturbed Fe|0.75 M H_2SO_4 system recorded in I=f(E) and I=f(t) curves is characterized by complex current oscillations. The halide concentration, c_X-, applied potential, *E* and time, all

affect characteristic features of oscillations, which point to pit initiation, propagation, and growth on an otherwise passive Fe surface.

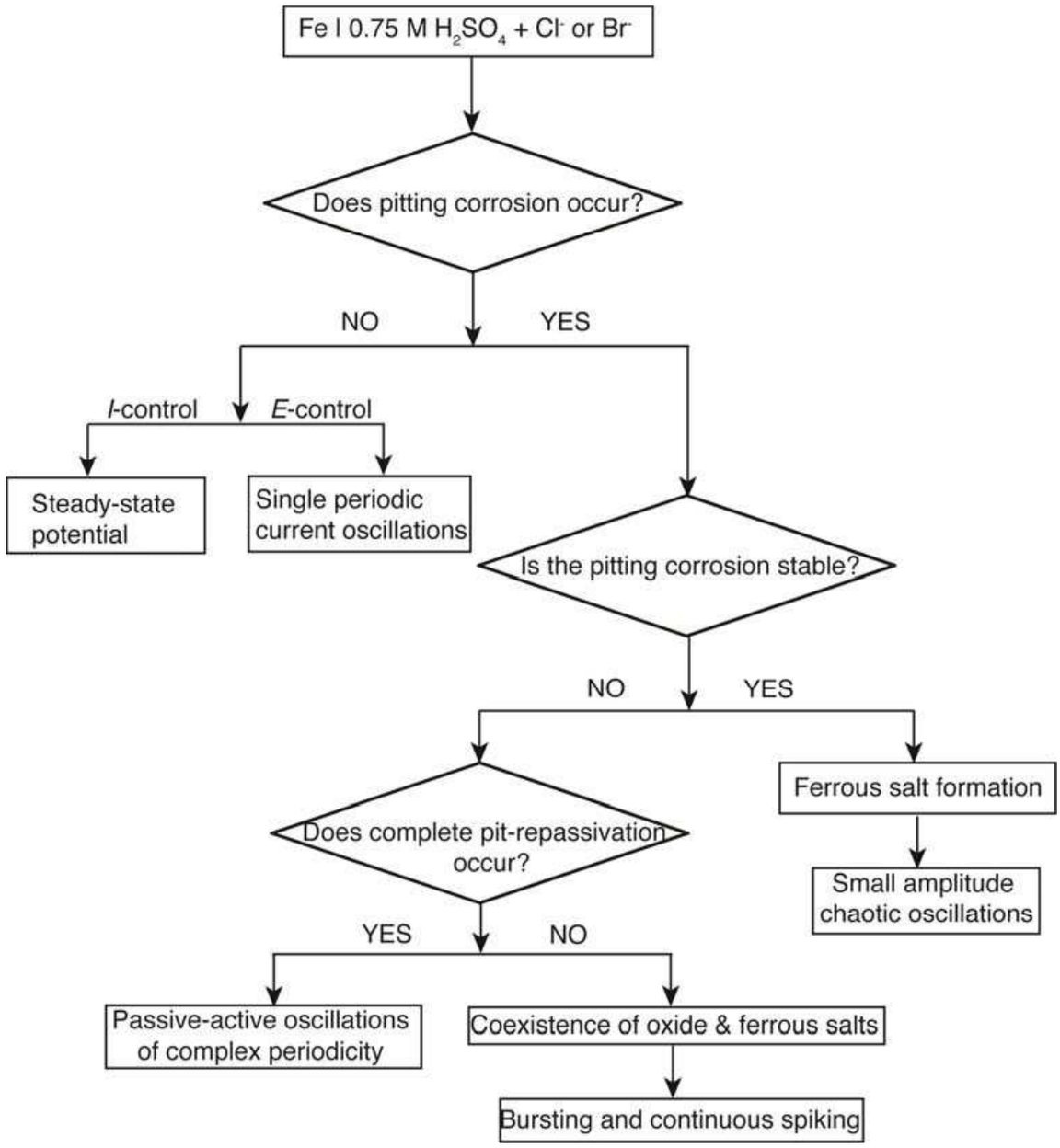

Fig. 15. Flow diagram displaying a phenomenological classification of the nonlinear dynamical response of the halide-perturbed Fe | 0.75 M H_2SO_4 system arisen at various stages of pitting corrosion.

Perturbation with relatively small amounts of Cl^- (c_{Cl^-} <20 mM) leads to unstable pitting corrosion associated with complex passive-active current oscillations arisen within a fixed potential region. These oscillations may be employed to distinguish between general and pitting corrosion and characterize pit initiation and propagation.

In summary, the localized breakdown of passivity on Fe and pit initiation are characterized by:

1. A gradual decrease of the current in the passive state, $I_{pas,f}$ and $I_{pas,b}$ upon increasing gradually the c_{Cl^-} .
2. No access to E_{tr} and the onset of E_{pit}. At potentials higher than E_{pit} a steady pit growth occurs.
3. The disappearance of the single periodic relaxation oscillation of the halide-free system and the onset of complex passive-active oscillations that represent early stages of pitting.
4. The induction time, t_{ind} elapsed before oscillations start. During t_{ind} pit nucleation and repassivation occur repeatedly.
5. Deviation of the $(I_{osc})_{max}$ from the kinetics of the linear part of the active region, which is assigned to the increase of the Fe active surface due to pitting.

Upon increasing c_{Cl^-}-> 20 mM and E the rate of pit growth is accelerated resulting in late stages of pitting corrosion. At late stages of pitting corrosion, formation of the iron oxide film becomes unlikely and precipitation of ferrous salts may occur. When a steady pit growth is established and formation of the oxide film becomes unlikely, the precipitation-dissolution of ferrous salt layers results in new oscillatory phenomena related to the following changes:

1. The current in the passive state tends to a limiting current value and a LCR emerges out of the passive state.
2. A critical pitting potential E_{pit} does not exist.
3. At lower potentials either aperiodic bursting oscillations or continuous spiking (beating) of the current (type I) are observed.
4. At higher potentials small amplitude chaotic oscillations (type II) arise around the LCR, instead of the large amplitude oscillations of type I. Beyond a halide concentration threshold, oscillations of type II occur within the entire oscillatory potential region.

Under current-controlled conditions, the nonlinear dynamical response of the halide-perturbed Fe|0.75 M H_2SO_4 system recorded in E=f(I) and E=f(t) curves is characterized by potential oscillations. It is worth-noting that under a current control the halide free-system exhibits only bistability without oscillations (Fig. 3b). Therefore, potential oscillations can be used alternatively to identify at a first glance pitting corrosion occurring at a critical c_{Cl^-} or c_{Br^-} that depends on the applied current. Iodides do not induce potential oscillations of this type due to the formation of a compact iodine surface layer. Potential oscillations recorded at different c_{Cl^-} or c_{Br^-} exhibit characteristic properties that correspond either to early or late stages of pits. In summary, identification and characterization of pitting corrosion should be based on the following criteria:

1. Onset of potential oscillations in the E = f(I) and E = f(t) curves.
2. The increase of the current I_{act} at which activation of Fe occurs during the backward current scan in the galvanodynamic E = f(I) curves upon increasing gradually either c_{Cl^-} or c_{Br^-}. The I_{act} coincides with the current in the passive state of the potentiodynamic I = f(E) curves and hence quantifies the extent of pitting corrosion and aggressiveness of halides.

3. The decrease of the induction period of time, t_{ind}, elapsed before potential oscillations start, upon increasing gradually either c_{Cl^-} and c_{Br^-} or I_{appl}. The t_{ind} characterizes the kinetics of pit initiation on the passive Fe surface.
4. The decrease of the average firing rate, $\langle r \rangle$ upon increasing gradually either c_{Cl^-} and c_{Br^-} or I_{appl}. The $\langle r \rangle$ characterizes pit growth and is associated with the conversion of the outermost oxide layer on the Fe surface to an unstable porous, nonprotective iron chloride or bromide ferrous salt film related rather to electropolishing state dissolution.

The formation of mutually interacted pits on the passive metal surface is necessary for the appearance of potential oscillations. An autocatalytic process formed by a coupling between the oxide detachment and oxide growth causes the repetitive passivation-activation processes resulting in the appearance of the potential oscillation (Sazou et al., 2009).

Analogous phenomena of current and potential oscillations have been also observed for other metals and certainly for several iron alloys during pitting corrosion (Podesta et al., 1979). Thus an approach within the framework of nonlinear dynamics might be used and further developed to study efficiently localized corrosion phenomena in other corroding systems.

8. Conclusions

Pitting corrosion is a complex multi-stage phenomenon of a great technological importance. It has been investigated intensively over many decades. Numerous theoretical and experimental contributions brought about considerable progress in understanding critical factors controlling pitting corrosion. Noticeable progress in elucidating pit nucleation processes during last decades might be attributed to the combined application of electrochemical and surface analytical techniques (Winston Revie, 2011). However, many aspects of pitting corrosion remain unclear.

In this brief review, an alternate route to investigate pitting corrosion is suggested. This includes a closer look on the conditions related to the onset of nonlinear dynamical response of the metal|electrolyte system as well as on characteristics of oscillations related to different stages of pitting. The halide-containing $Fe|H_2SO_4$ system was selected as a paradigm using current oscillations observed under potentiostatic conditions as well as potential oscillations observed under galvanostatic conditions. Since oscillatory phenomena is a widespread phenomenon in electrochemical reactions, many other metal|electrolyte systems should certainly respond by an oscillatory current and/or potential to a halide ion perturbation. A wide variety of processes can lead to oscillation in the current and potential.

In the case of the halide-perturbed $Fe|H_2SO_4$ system these processes can be classified at first in two broad categories, those associated with general corrosion and those associated with pitting corrosion. General corrosion corresponds to either a stable steady-state passivity under current- controlled conditions or single periodic current oscillations under potential-controlled conditions. Pitting corrosion corresponds to complex periodic and aperiodic (bursting and continuous spiking) oscillation. Second, processes associated with pitting corrosion can be distinguished to those leading to early stages of pitting and those leading to late stages. At early stages, unstable pitting gives rise to passive-active current and potential oscillation. Both current and potential oscillate between the active state (high

current, low potential) and the passive state (low current, high potential). At late stages, the oxide growth becomes unlikely and stable pitting evolves through the precipitation-dissolution of ferrous salt layers whereas complex current or potential oscillations arise. Quantities such as the dissolution current, the induction period required for oscillation to occur and the frequency of oscillations can describe the kinetics of different processes.

It is also worth noting, that current transients of a stochastic nature (noise) of the order of μA might be also induced by halide ions due to randomly nucleated metastable pits over the passive metal surfaces. They occur at potentials lower than the E_{pit}, being the critical potential for pit stabilization. Spatial and temporal interactions among metastable pits leading to clustering and hence high corrosion rates of stainless steel were investigated thoroughly over last decade within the context of nonlinear dynamics and pattern formation (Lunt et al., 2002; Mikhailov et al., 2009; Organ et al., 2005; Punckt et al., 2004). The potential region where these current transients appear is distinctly different from the potential region within which the large-amplitude complex passive-active current oscillations, discussed in this article, arise. Both stochastic noise and deterministic oscillations can be useful in investigating localized corrosion, which is by itself a typical intrinsically complex system (Aogaki, 1999).

This brief review, not necessarily comprehensive, has focused on results from a research project being carried out by our research group over last two decades. It is noticeable that complex and chaotic current or potential oscillations can be further analyzed using numerical diagnostics (i.e. power spectral density, phase portraits, correlation dimension of chaotic attractors, Lyapunov exponents) developed to characterize time series in nonlinear dynamical systems (Corcoran & Sieradzki, 1992; Hudson & Basset, 1991; Kantz & Schreiber, 1997; Karantonis & Pagitsas, 1996; Li et al., 2005; Li et al., 1993). This analysis might provide new diagnostic criteria that can be profitably used in pitting corrosion studies. However, the purpose of this chapter was restricted to point out the rich dynamical response that may arise under appropriate conditions when localized breakdown of the passivity on a metal occurs. It seems that the need for continuing research into the field remains mandatory. It is our belief that the rich nonlinear dynamical response of corrosive systems can be used profitably to gain a further understanding of complex, not-fully understood processes underlying technologically important problems.

9. References

Aogaki, R., Nonequilibrium fluctuations in the corrosion process. In: E. White, et al., (Eds.), *Modern Aspects of Eelctrochemistry*. Plenum Publishers, N.Y., 1999, Vol. 33, pp. 217-305.

Berthier, F., Diard, J.-P., Gorrec, B. L., Montella, C. (2004) Study of the forced Ni|1 M H_2SO_4 oscillator. *J. Electroanal. Chem.*, 572**,** 267-281.

Birzu, A., Green, B. J., Jaeger, N. I., Hudson, J. L. (2001) Spatiotemporal patterns during electrodissolution of a metal ring:three-dimensional simulations. *J. Electroanal. Chem.*, 504**,** 126-136.

Birzu, A., Green, B. J., Otterstedt, R. D., Jaeger, N. I., Hudson, J. L. (2000) Modelling of spatiotemporal patterns during metal electrodissolution in a cell with a point reference electrode. *Phys. Chem. Chem. Phys*, 2**,** 2715-2724.

Bohni, H., Localized corrosion. In: F. Mansfeld, (Ed.), *Corrosion Mechanisms*. Marcel Dekker, NY, 1987, pp. 285-328.

Budiansky, N. D., Hudson, J. L., Scully, J. R. (2004) Origins of persistent interaction among localized corrosion sites on stainless steel. *J. Electrochem. Soc.*, 151**,** B233-B243.

Corcoran, S. G., Sieradzki, K. (1992) Chaos during the growth of an artificial pit. *J. Electrochem. Soc.*, 139**,** 1568-1573.

Dayan, P., Abbott, B., 2001. *Theoretical Neuroscience, Computational and Mathematical Modeling of Neural Systems*. The MIT Press, Cambridge, Massachusetts.

Eiswirth, M., Lubke, M., Krischer, K., Wolf, W., Hudson, J. L., Ertl, G. (1992) Structural effects on the dynamics of an electrocatalytic oscillator. *Chem. Phys. Lett.,* 192**,** 254-258.

Engell, H. J. (1977) Stability and breakdown phenomena of passivating films. *Electrochim. Acta*, 22**,** 987-993.

Ertl, G. (1998) Pattern formation at electrode surfaces. *Electrochim. Acta*, 43**,** 2743-2750.

Ertl, G. (2008) Reactions at surfaces: from atoms to complexity (Nobel lectrure). *Angew. Chem. Int. Ed.*, 47**,** 3524-3535.

Fechner, G. T. (1828) Zur Elektrochemie-I. Uber Umkehrungen der Polaritat in der einfachen Kette. *Schwigg J Chem. Phys.* , 53**,** 129.

Franck, U. F. (1978) Chemical oscillations. *Angew. Chem. Int. Ed.* , 17**,** 1-15.

Franck, U. F., Fitzhugh, R. (1961) Periodische Elektrodenprozesse Und Ihre Beschreibung Durch Ein Mathematisches Modell. *Z. Elektrochemie*, 65**,** 156-168.

Frankel, G. S. (1998) Pitting corrosion of metals. A review of the critical factors. *J. Electrochem. Soc.*, 145**,** 2186-2198.

Fujioka, E., Nishihara, H., Aramaki, K. (1996) The inhibition of pit nucleation and growth on the passive surface of iron in a borate buffer solution containing Cl- by oxidizing inhibitors. *Corros. Sci.*, 38**,** 1915-1933.

Gabrielli, C., Keddam, M., Stupnisek-Lisac, E., Takenouti, H. (1976) Etude du comportment anodique de interface fer-acid nitrique a l'aide d'une regulation a resistance negative *Electrochim. Acta*, 21**,** 757-766.

Georgolios, C., Sazou, D. (1998) On the mechanism initiating bursting oscillatory patterns during the pitting corrosion of a passive rotating iron-disc electrode in halide-containing sulphuric acid solutions. *J. Solid State Electrochem.*, 2**,** 340-346.

Geraldo, A. B., Barcia, O. E., Mattos, O. R., Huet, F., Tribollet, B. (1998) New results concerning the oscillations observed for the system iron-sulphuric acid. *Electrochim. Acta*, 44**,** 455-465.

Green, B. J., Hudson, J. L. (2001) Spatiotemporal patterns and symmetry breaking on a ring electrode. *Phys. Rev. E*, 63**,** 0226214-1-0226214-8.

Hudson, J. L., Basset, M. R. (1991) Oscilaltory eelctrodissolution of metals. *Rev. Chem. Eng.*, 7**,** 102-109.

Hudson, J. L., Krischer, J. T., Kevrekidis, I. G. (1993) Spatiotemporal period doubling during the electrodissolution of iron. *Phys. Lett. A*, 179**,** 355-363.

Hudson, J. L., Tsotsis, T. T. (1994) Electrochemical reaction dynamics. A review. *Chem. Eng. Sci.*, 49**,** 1493-1572.

Janik-Czachor, M. (1981) An assessment of the processes leading to pit nucleation on iron. *J. Electrochem. Soc.*, 128**,** 513C-519C.

Kaesche, H., 1986. *Metallic Corrosion*. NACE, TX.

Kantz, H., Schreiber, T., 1997. *Nonlinear Time Series Analysis*. Cambridge University Press, Cambridge, U.K.

Karantonis, A., Pagitsas, M. (1996) Comparative study for the calculation of the Lyapunov spectrum from nonlinear experiemntal signals. *Phys. Rev. E*, 53**,** 5428-5444.

Karantonis, A., Pagitsas, M. (1997) Constructing normal forms from experimental observations and time series analysis. *Int. J. Bif. Chaos*, 7**,** 107-127.

Karantonis, A., Pagitsas, M., Miyakita, Y., Nakabayashi, H. (2005) Manipulation of spatio-temporal patterns in networks of relaxation electrochemical oscillators. *Electrochim. Acta*, 50**,** 5056-5064.

Karantonis, A., Shiomi, Y., Nakabayashi, S. (2000) Coherence and coupling during oscillatory metal electrodissolution. *J. Electroanal. Chem.*, 493**,** 57-67.

Keddam, M., Lizee, J. F., Pallotta, C., Takenouti, H. (1984) Electrochemical behavior of passive iron in acid medium. 1. Impedance approach. *J. Electrochem. Society*, 131**,** 2016-2024.

Kiss, I. Z., Hudson, J. L. (2003) Chaotic cluster itirenancy and hierarchical cluster trees in electrochemical experiments. *Chaos*, 13**,** 999-1009.

Kiss, I. Z., Hudson, J. L., Santos, G. J. E., Parmananda, P. (2003) Experiments on coherence resonance: Noisy precursors to Hopf bifurcations. *Phys. Rev. E*, 67**,** 035201-035204.

Kiss, I. Z., Lv, Q., Organ, L., Hudson, J. L. (2006) Electrochemical bursting oscillations on a high-dimensional slow subsystem. *Phys. Chem. Chem. Phys.*, 8**,** 2707-2715.

Kleinke, M. U. (1995) Chaotic behavior of current oscillations during iron electrodissolution in sulfuric acid. *J. Phys. Chem. B*, 99**,** 17403-17409.

Koper, M. T. M., Oscillation and complex dynamical bifurcation in electrochemical systems. In: I. Prigogine, S. A. Rice, (Eds.), *Adv. Chem. Phys.* Wiley, N.Y., 1996a, Vol. XCII, pp. 161-298.

Koper, M. T. M. (1996b) Stability study and categorization of electrochemical oscillators by impedance spectroscopy. *J. Electroanal. Chem.*, 409**,** 175-182.

Koper, M. T. M., Sluyters, J. H. (1993a) A mathematical model for current oscillations at the active-passive transition in metal electrodissolution. *J. Electroanal. Chem.*, 347**,** 31-48.

Koper, M. T. M., Sluyters, J. H. (1993b) On the mathematical unification of a class of electrochemical oscillators and their design procedures. *J. Electroanal. Chem.*, 352**,** 51-64.

Koutsaftis, D., Karantonis, A., Pagitsas, M., Kouloumbi, N. (2007) Transient and persistent electrochemical bursting induced by halide ions. *J. Phys. Chem. C*, 111**,** 13579-13585.

Krischer, K., Principles of temporal and spatial formation in electrochemical systems. In: R. E. White, et al., (Eds.), *Modern Aspects of Electrochemistry*. Kluwer Academic/Plenum Publishers, NY, 1999, Vol. 32, pp. 1-142.

Krischer, K., Nonlinear dynamics in electrochemical systems. In: R. C. Alkire, D. M. Kolb, (Eds.), *Advances in Electrochemical Sciences and Engineering*. Wiley-VCH Verlag GMbH & Co. KgaA, Weinheim, 2003b, Vol. 8, pp. 89-208.

Lev, O., Wolffberg, A., Pismen, L. M. (1988) Bifurcations to periodic and chaotic motions in anodic nickel dissolution. *Chem. Eng. Sci.*, 43**,** 1339-1353.

Li, L., Luo, J. L., Lu, B. T., Chen, S. H. (2005) Effect of interface chloride ion perturbation on oscillatory electrodissolution. *Electrochim. Acta*, 50**,** 3524-3535.

Li, W. H., Nobe, K. (1993) Electrodissolution kinetics of iron in chloride solutions .9. Effect of benzotriazole on potential oscillations. *J. Electrochem. Soc.*, 140**,** 1642-1650.

Li, W. H., Nobe, K., Pearlstein, A. J. (1993) Electrodissolution kinetics of iron in chloride solutions .VIII. Chaos in potential/current oscillations. *J. Electrochem. Soc.*, 140**,** 721-728.

Li, W. H., Wang, X. L., Nobe, K. (1990) Electrodissolution kinetics of iron in chloride solution. 7. Experimental potential/current oscillations. *J. Electrochem. Soc.*, 137**,** 1184-1188.

Lunt, T. T., Scully, J. R., Brusamarello, V., Mikhailov, A. S., Hudson, J. L. (2002) Spatial interactions among localized corrosion sites. Experiments and modeling. *J. Electrochem. Soc.*, 2002**,** B163-B173.

Ma, H.-Y., Yin, B.-S., Li, G.-Y., Guo, W.-J., Chen, S.-H., Tang, K. (2003) A study of the relation between current oscillations and pitting. *Chin. J. Chem.*, 21**,** 1309-1314.

Ma, L., Vitt, J. E. (1999) Current oscillations during iodide oxidation at a gold rotating disk electrode. *J. Electrochem. Soc.*, 146**,** 4152-4157.

Macdonald, D. D. (1992) The point defect model for the passive state. *J. Electrochem. Soc.*, 139**,** 3434-3449.

Maurice, V., Marcus, P., Scanning tunneling microscopy and atomic force microscopy. In: P. Marcus, F. Mansfeld, (Eds.), *Analytical Methods in Corrosion Science and Engineering*. CRC Press, Taylor & Francis Group, N.Y., 2006, pp. 133-168.

Mikhailov, A. S., Scully, J. R., Hudson, J. L. (2009) Nonequilibrium collective phenomena in the onset of pitting corrosion. *Surf. Sci.*, 603**,** 1912-1921.

Nakanishi, S., Sakai, S., Nagai, T., Nakato, Y. (2005) Macroscopically uniform nanoperiod alloy multilayers formed by coupling of electrodeposition with current oscillations. *J. Phys. Chem. B*, 109**,** 1750-1755.

Newmann, R. C., Ajjawi, M. A. A. (1986) A micro-electrode study of the nitrate effect on pitting of stainless steel. *Corros. Sci.*, 26**,** 1057-1063.

Organ, L., Sculli, J., Mikhailov, A. S., Hudson, J. L. (2005) A spatiotemporal model of interactions among metastable pits and the transition to pitting corrosion. *Electrochim. Acta*, 51**,** 225-241.

Orlik, M. (2009) Self-organization in nonlinear dynamical systems and its relation to the materials science. *J. Solid State Electrochem.*, 13**,** 245-261.

Otterstedt, R. D., Plath, P. J., Jaeger, N. I. (1996) Modulated electrochemical waves. *Phys. Rev. E*, 54**,** 3744-3751.

Pagitsas, M., Diamantopoulou, A., Sazou, D. (2001) Distinction between general and pitting corrosion based on the nonlinear dynamical response of passive iron surfaces perturbed chemically by halides. *Electrochem. Commun.*, 3**,** 330-335.

Pagitsas, M., Diamantopoulou, A., Sazou, D. (2002) General and pitting corrosion deduced from current oscillations in the passive-active transition state of the $Fe|H_2SO_4$ electrochemical system. *Electrochim. Acta*, 47**,** 4163-4179.

Pagitsas, M., Diamantopoulou, A., Sazou, D. (2003) A point defect model for the general and pitting corrosion on iron|oxide|electrolyte interface deduced from current oscillations. *Chaos Solit. & Fractals*, 17**,** 263-275.

Pagitsas, M., Pavlidou, M., Papadopoulou, S., Sazou, D. (2007) Chlorates induce pitting corrosion of iron in sulfuric acid solutions: An analysis based on current oscillations and a point defect model. *Chem. Phys. Lett.*, 434**,** 63-67.

Pagitsas, M., Pavlidou, M., Sazou, D. (2008) Localized passivity breakdown of iron in chlorate- and perchlorate-containing sulphuric acid solutions: A study based on current oscillations and a point defect model. *Electrochim. Acta*, 53**,** 4784-4795.

Pagitsas, M., Sazou, D. (1991) The improved Franck-Fitzhugh model for the electrodissolution of iron in sulfuric-acid-solutions. Linear stability and bifurcation analysis. Derivation of the kinetic equations for the forced Franck-Fitzhugh model. *Electrochim. Acta*, 36**,** 1301-1308.

Pagitsas, M., Sazou, D. (1999) Current oscillations induced by chlorides during the passive-active transition of iron in a sulfuric acid solution. *J. Electroanal. Chem.*, 471**,** 132-145.

Parmananda, P., Rivera, M., Madrigal, R. (1999) Altering oscillatory dynamics of an electrochemical system using external forcing. *Electrochim. Acta*, 44**,** 4677-4683.

Parmananda, P., Rivera, M., Madrigal, R., Kiss, I. Z., Gaspar, V. (2000) Resonant control of electrochemical oscillations. *J. Phys. Chem. B*, 104**,** 11748-11751.

Pickering, H. W. (1989) The significance of the local electrode potential within pits, crevices and cracks. *Corros. Sci.*, 29**,** 325-341.

Pickering, H. W., Frankenthal, R. P. (1972) On the mechanism of localized corrosion of iron and stainless steel. I. Electrochemical studies. *J. Electrochem. Soc.*, 119**,** 1297-1303.

Podesta, J. J., Piatti, R. C. V., Arvia, A. J. (1979) Potentiostatic current oscillations at iron/sulphuric acid solution interfaces. *J. Electrochem. Soc.*, 126**,** 1363-1367.

Postlethwaite, J., Kell, A. (1972) Periodic phenomena during the anodic dissolution of iron in sodium chloride solutions. *J. Electrochem. Soc.*, 119**,** 1351-1352.

Punckt, C., Bolscher, M., Rotermund, H. H., Mikhailov, A. S., Organ, L., Budiansky, N. D., Scully, J. R., Hudson, J. L. (2004) Sudden onset of pitting corrosion on stainless steel as a critical phenomenon. *Science*, 305**,** 1133-1135.

Rius, A., Lizarbe, R. (1962) Study of the anodic behavior of iron at high potentials in solutions containing chloride ions. *Electrochim. Acta*, 7**,** 513-422.

Rush, B., Newman, J. (1995) Periodic behavior in the iron sulfuric-acid system. *J. Electrochem. Soc.*, 142**,** 3770-3779.

Saitou, M., Fukuoka, Y. (2004) An experimental study on stripe pattern formation of Ag-Sb electrodeposits. *J. Phys. Chem. B*, 108**,** 5380-5385.

Sato, N. (1982) Anodic breakdown of passive films on metals. *J. Electrochem. Soc.*, 129**,** 255-260.

Sato, N. (1987) Some concepts of corrosion fundamentals. *Corros. Sci.*, 27**,** 421-433.

Sato, N. (1989) Toward a more fundamental understanding of corrosion processes. *Corrosion*, 45**,** 354-368.

Sato, N. (1990) An overview on the passivity of metals. *Corros. Sci.*, 31**,** 1-19.

Sazou, D., Diamantopoulou, A., Pagitsas, M. (2000a) Chemical perturbation of the passive-active transition state of Fe in a sulfuric acid solution by adding halide ions. Current oscillations and stability of the iron oxide film. *Electrochim. Acta*, 45**,** 2753-2769.

Sazou, D., Diamantopoulou, A., Pagitsas, M. (2000b) Complex periodic and chaotic current oscillations related to different states of the localized corrosion of iron in chloride-containing sulfuric acid solutions. *J. Electroanal. Chem.*, 489**,** 1-16.

Sazou, D., Diamantopoulou, A., Pagitsas, M. (2000c) Conditions for the onset of current oscillations at the limiting current of the iron electrodissolution in sulfuric acid solutions. *Russ. J. Electrochem.*, 36**,** 1072-1084.

Sazou, D., Karantonis, A., Pagitsas, M. (1993a) Generalized Hopf, saddle-node infinite period bifurcations and excitability during the electrodissolution and passivation of iron in a sulfuric acid solution. *Int. J. Bif. Chaos*, 3**,** 981-997.

Sazou, D., Pagitsas, M. (2002) Nitrate ion effect on the passive film breakdown and current oscillations at iron surfaces polarized in chloride-containing sulfuric acid solutions. *Electrochim. Acta*, 47**,** 1567-1578.

Sazou, D., Pagitsas, M. (2003a) Electrochemical current oscillations during localized corrosion of iron. *Fluct. & Noise Lett.*, 3**,** L433-L454.

Sazou, D., Pagitsas, M. (2003b) Non-linear dynamics of the passivity breakdown of iron in acidic solutions. *Chaos Solit. & Fractals*, 17**,** 505-522.

Sazou, D., Pagitsas, M. (2006a) Electrochemical instabilities due to pitting corrosion of iron. *Russ. J. of Electrochem.*, 42**,** 476-490.

Sazou, D., Pagitsas, M. (2006b) On the onset of current oscillations at the limiting current region emerged during iron electrodissolution in sulfuric acid solutions. *Electrochim. Acta*, 51**,** 6281-6296.

Sazou, D., Pagitsas, M., Geogolios, C. (1993b) Bursting and beating current oscillatory phenomena induced by chloride-ions during corrosion/passivation of iron in sulfuric acid solutions. *Electrochim. Acta*, 38**,** 2321-2332.

Sazou, D., Pagitsas, M., Georgolios, C. (1992) The influence of chloride-ions on the dynamic characteristics observed at the transition between corrosion and passivation states of an iron electrode in sulfuric acid solutions. *Electrochim. Acta*, 37**,** 2067-2076.

Sazou, D., Pavlidou, E., Pagitsas, M. (2011) Potential oscillations induced by localized breakdown of the passivity on Fe in halide-containing sulphuric acid media as a probe for a comparative study of the halide ion effect. *submitted*.

Sazou, D., Pavlidou, M., Pagitsas, M. (2009) Temporal patterning of the potential induced by localized corrosion of iron passivity in acid media. Growth and breakdown of the oxide film described in terms of a point defect model. *Phys. Chem. Chem. Phys.*, 11**,** 8841-8854.

Schmuki, P. (2002) From Bacon to barriers: a review on the passivity of metals and alloys. *J. Solid State Electrochem.*, 6**,** 145-164.

Schultze, J. W., Lohrenger, M. M. (2000) Stability, reactivity and breakdown of passive films. Problems of recent and future research. *Electrochim. Acta*, 45**,** 2499-2513.

Strehblow, H. H., Mechanisms of pitting corrosion. In: P. Marcus, J. Oudar, (Eds.), *Corrosion Mechanisms in Theory and Practice*. Marcel Dekker, NY, 1995, pp. 201-237.

Strehblow, H. H., Wenners, J. (1977) Investigation of processes on iron and nickel electrodes at high corrosion current densities in solutions of high chloride content. *Electrochim. Acta*, 22**,** 421-427.

Taveira, L. V., Macak, J. M., Sirotna, K., Dick, L. F. P., Schmuki, P. (2006) Voltage oscillations and morphology during the galvanostatic formation of self-organized TiO_2 nanotubes. *J. Electrochem. Soc.*, 153**,** B137-B143.

Toney, M. F., Davenport, A. J., Oblonsky, L. J., Ryan, M. P., Vitus, C. M. (1997) Atomic structure of the passive oxide film formed on iron. *Phys. Rev. Lett.*, 79**,** 4282-4285.

Vetter, K. J. (1971) General kinetics of passive layers on metals. *Electrochim. Acta*, 16**,** 1923-1937.

Vitt, J. E., Johnson, D. C. (1992) The importance of anodic discharge of H_2O in anodic oxygen-transfer reactions. *J. Electrochem. Soc.*, 139**,** 774-778.

Wang, C., Chen, S. (1998) Holographic microphotography study of periodic electrodissolution of iron in a magnetic field. *Electrochim. Acta*, 43**,** 2225-2232.

Wang, C., Chen, S., Yang, X., Li, L. (2004) Investigation of chloride-induced pitting processes of iron in the H_2SO_4 solution by the digital holography. *Electrochem. Commun.*, 6**,** 1009-1015.

Winston Revie, R., 2011. *Uhlig's Corrosion Handbook*. John Wiley & Sons, Inc. , N.J., U.S.A.

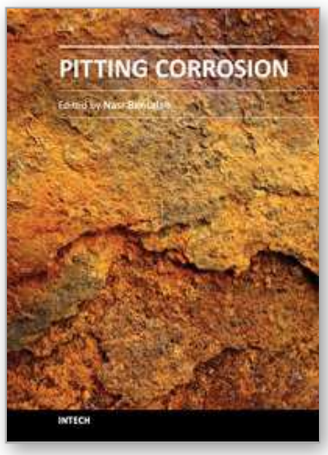

Pitting Corrosion

Edited by Prof. Nasr Bensalah

ISBN 978-953-51-0275-5
Hard cover, 178 pages
Publisher InTech
Published online 23, March, 2012
Published in print edition March, 2012

Taking into account that corrosion is costly and dangerous phenomenon, it becomes obvious that people engaged in the design and the maintenance of structures and equipment, should have a basic understanding of localized corrosion processes. The Editor hopes that this book will be helpful for researchers in conducting investigations in the field of localized corrosion, as well as for engineers encountering pitting and crevice corrosion, by providing some basic information concerning the causes, prevention, and control of pitting corrosion.

How to reference

In order to correctly reference this scholarly work, feel free to copy and paste the following:

Dimitra Sazou, Maria Pavlidou, Aggeliki Diamantopoulou and Michael Pagitsas (2012). Oscillatory Phenomena as a Probe to Study Pitting Corrosion of Iron in Halide-Containing Sulfuric Acid Solutions, Pitting Corrosion, Prof. Nasr Bensalah (Ed.), ISBN: 978-953-51-0275-5, InTech, Available from: http://www.intechopen.com/books/pitting-corrosion/oscillatory-phenomena-as-a-probe-to-study-pitting-corrosion-of-iron-in-halide-containing-sulfuric-ac

INTECH
open science | open minds

InTech Europe
University Campus STeP Ri
Slavka Krautzeka 83/A
51000 Rijeka, Croatia
Phone: +385 (51) 770 447
Fax: +385 (51) 686 166
www.intechopen.com

InTech China
Unit 405, Office Block, Hotel Equatorial Shanghai
No.65, Yan An Road (West), Shanghai, 200040, China
中国上海市延安西路65号上海国际贵都大饭店办公楼405单元
Phone: +86-21-62489820
Fax: +86-21-62489821

IntechOpen